VALIDATION OF THE CQUAD4 ELEMENT FOR VIBRATION AND SHOCK ANALYSIS OF THIN LAMINATED COMPOSITE PLATE STRUCTURE

by

Douglas E. Lesar
Ship Structures and Protection Department
Carderock Division, Naval Surface Warfare Center
Bethesda, Maryland 20084-5000 U.S.A.

ABSTRACT

The CQUAD4 thin plate element implemented in COSMIC NASTRAN is capable of modeling thin layered plate and shell structures composed of orthotropic lamina. Fiber-reinforced composites are among the classes of inhomogeneous and non-isotropic materials which can be treated. Although the CQUAD4 has been extensively checked in static cases, little validation has been carried out for vibration response modeling. This paper documents validation of the CQUAD4 element's accuracy for vibration response analysis of thin laminated composite plates.

The lower-order natural frequencies and mode shapes of ten glass fiber-reinforced plastic (GFRP) and carbon fiber-reinforced plastic (CFRP) plates are computed and compared to published experimental and numerically-computed data. A range of ply geometries including unidirectional, cross-ply, and angle-ply are considered. The plates' length-to-thickness ratios all lie in the vicinity of 100 to 150. The CQUAD4 plate idealizations provide natural frequency predictions within ten percent of measured data for all six lowest modes of seven of ten plates. For two of the remaining three plates, only the fundamental frequency is predicted with an error greater than ten percent. Results for the one remaining plate do not correlate with published data, possibly because of erroneous reporting of its geometry or material properties in the literature. To obtain accurate frequency predictions, lamina in-plane elastic moduli had to be tuned to reflect each plate's fiber volume fraction.

These results show that the NASTRAN CQUAD4 plate element is useful and reasonably accurate for vibration and shock analysis of structures composed of thin fiber-reinforced plastic plates.

INTRODUCTION

There is strong current Navy interest in exploitation of fiber-reinforced plastics as lightweight materials for a wide variety of ship structures. These structures must be designed to withstand in-service loads of quasi-static, transient dynamic, and steady-state dynamic nature. For many ship structures, transient shock is a primary load. For these and others, steady-state vibration response

impacts the ship's acoustic signature. In both cases, the structure's modal properties (natural frequencies, mode shapes, and modal loss factors) are key parameters governing its transient and steady-state response. In most cases, the ship structures being designed are complex enough so that numerical (finite element) methods must be employed to obtain realistic modal property estimations.

The NASTRAN finite element code is one of the Navy's premier tools for steady-state vibration response analysis of ship and submarine structures. Undamped natural mode analysis and forced vibration response analysis with hysteretic damping can be performed by NASTRAN, as well as modal frequency and loss factor analysis for structures with viscoelastic damping materials (Ref. 1). NASTRAN is also a key component of the NASHUA suite of codes for performing radiated noise and acoustic scattering analysis of vibrating submerged structures (Ref. 2,3).

The COSMIC NASTRAN CQUAD4 element is designed to model anisotropic layered plates as well as homogeneous and isotropic plates. The theory and assumptions behind the CQUAD4 have been informally documented (Ref. 4). The CQUAD4 has been found to be more accurate for a given finite element grid than its predecessor, the CQUAD2 element, for prediction of low frequency eigenmodes of thin-walled cylindrical shells composed of isotropic materials (Ref. 5). To the author's knowledge, no comparable study of the accuracy of the CQUAD4 formulation for anisotropic plate or shell vibration yet exists, particularly for plates and shells composed of layers of fiber-reinforced plastic lamina.

This paper summarizes an investigation of the accuracy of the NASTRAN CQUAD4 membrane and plate bending element for vibration analysis of structures composed of thin fiber-reinforced composite plates. This is accomplished by comparisons of NASTRAN-computed undamped natural frequencies of ten GFRP and CFRP plates with published experimental data and other numerical predictions.

NOTATION

E_{11}	Lamina extensional modulus in direction parallel with fibers
E_{22}	Lamina extensional modulus in direction transverse to fibers
E_{33}	Through-thickness extensional modulus
G_{12}	In-plane lamina shear modulus
G_{13}	Transverse lamina shear modulus for out-of-plane shearing of a fiber cross section

G_{23}	Transverse lamina shear modulus for in-plane shearing of a fiber cross section
L	Plate side length
t	Plate thickness
v_f	Fiber volume fraction
γ_{12}	In-plane shear strain
γ_{13}, γ_{23}	Out-of-plane shear strains
ϵ_1, ϵ_2	In-plane extensional strains
θ	Fiber orientation angle with respect to one plate side
ν_{12}, ν_{21}	In-plane lamina Poisson's ratios
ν_{23}	Transverse lamina Poisson's ratio
ρ	Average mass density
σ_1, σ_2	In-plane extensional stresses
τ_{12}	In-plane shear stress
τ_{13}, τ_{23}	Out-of-plane shear stresses

ABBREVIATIONS

avg.	Average
CFRP	Carbon fiber-reinforced plastic
CLT	Classical lamination theory
consis.	Consistent
CPT	Classical plate theory
DOF	Degree(s)-of-freedom
FEA	Finite Element Analysis
GPa	Gigapascals
GFRP	Glass fiber-reinforced plastic
Hz	Hertz
kg	Kilograms

m	Meters
mm	Millimeters
params.	Parameters
psi	Pounds (force) per square inch
ref.	Reference(s)
RMS	Root-mean-square
sym	Midplane-symmetric

BACKGROUND

Anisotropic plate analysis is more difficult and involves more variables and parameters than isotropic plate analysis. The importance of accounting for transverse shear flexibility in relatively thin composite laminates is discussed in the next section. The ways by which the CQUAD4 addresses these difficulties are also briefly described.

TRANSVERSE SHEAR DEFORMATION ISSUES

In composite plate mechanics, the counterpart of the well-known Kirchhoff (Classical plate) theory (CPT) for isotropic plates is the so-called "Classical Lamination Theory" (CLT). The two theories invoke the same kinematic assumptions regarding the deformation of the plate with respect to its middle surface; that is, sections originally planar and perpendicular to the middle surface remain planar and perpendicular in the deformed state. The mathematical development of CLT occupies much of the text by Jones (Ref. 6). The reader should consult this (or some other) text for detailed exposition of CLT assumptions and derivation of the CLT equations.

The accuracy of the Kirchhoff kinematic assumption in isotropic plate mechanics degrades when the plate thickness becomes significant compared to its span length. For isotropic metallic plates, transverse shear-stiffness-governed transverse deflection becomes significant relative to flexural deflection when the span length-to-thickness ratio (L/t) is sufficiently small. An idea of required smallness can be gained from the discussion of "corrected" plate flexural waves in Chapter II, Section 3b of Cremer, Heckl, and Ungar (Ref. 7). They show, for a uniformly thick plate composed of an <u>isotropic</u> material, that transverse shear effects decrease flexural wavespeed by ten percent when the flexural wavelength is about six times the plate thickness. For one-half wavelength over a plate span length, this limitation translates to an L/t ratio of 3.

In the case of high modulus composite plates, an analogous limitation of the adequacy of CLT is encountered at <u>larger</u> L/t. This more stringent limit arises because the ratio of effective laminate extensional elastic modulus to shear modulus is a key fac-

tor (other than section geometry) governing the magnitude of shear deformation relative to flexure. A rough idea of limiting L/t ratios for the adequacy of CLT for composite plates follows from insertion of some "ballpark" ratios of effective laminate extensional and transverse shear moduli for GFRP and CFRP into the approximate expression for shear-corrected plate flexural wavespeed found on page 115 of Reference 7. Using E_{11} / G_{23} = 13 for GFRP and 125 for CFRP, ten percent differences in wavespeed arise for L/t of 6.75 and 20.9, respectively. (A comparable modulus ratio for isotropic materials is 2.6). These ad hoc assessments are qualitatively corroborated by static examples found in section 6.5 of Reference 6. In the problem of cylindrical bending of a CFRP strip with E_{11} / G_{23} = 125, maximum static deflection predicted by CLT is twenty percent smaller than the true shear-corrected solution at L/t = 20.

The low frequency composite plate vibration literature is dominated by evaluation of methods for account of transverse (interlaminar) shear in prediction of natural vibration frequencies and modal deflections. The inadequacies of CLT even for fundamental plate frequencies are repeatedly demonstrated in the literature for L/t's of 5 or 10. Many approaches have been developed to provide finite element-based plate formulations to handle through-thickness stress fields for arbitrary L/t. In these complex formulations, transverse normal stresses are no longer assumed to be zero, transverse shear stresses are constrained to be zero on upper and lower laminate surfaces, and shear stress continuity between laminae is maintained. As a result, sections perpendicular to the plate midplane rotate with respect to the midplane and warp out of a planar configuration.

The plate finite elements simulating through-thickness stress fields in laminates are, obviously, quite sophisticated. Tables III and VI of Mallikarjuna and Kant (Ref. 8) provide a good flavor for the performance of some higher-order approaches for reckoning with the effect of transverse shear and normal strains in plate vibration frequency prediction. Table III shows that CLT provides reasonable fundamental frequency predictions for a simply-supported CFRP angle-ply plate for L/t at and above 20. Even for such highly anisotropic plates, the complications of very complex high-order transverse shear theories, necessary for laminate strength and structural integrity problems, are not justified in vibration problems unless L/t is less than about 20, or if short-wavelength (high frequency) vibration modes are of interest.

The NASTRAN CQUAD4 membrane and bending element embodies the assumptions of CLT, but contains first-order corrections for transverse shear flexibility. When the CQUAD4 is used to model homogeneous plates, transverse shear strains vary linearly with the thickness coordinate, and zero shear stress and strain boundary conditions on upper and lower plate surfaces are not satisfied. The shear energy implied by the linear distribution is corrected by a multiplicative constant to produce the energy implied by the true quadratic distribution. As a result of these assumptions, sections perpendicular to the plate midplane are allowed to rotate with

respect to the midplane, but remain straight when the plate is in the deflected state. This ad hoc transverse shear correction extends the element's range of validity to thicker homogeneous plates, but is not acceptable for inhomogeneous layered plates.

When modeling inhomogeneous plates composed of orthotropic layers, a quadratic transverse shear strain distribution is assumed in each layer of the CQUAD4 element. Interlaminar shear strains are matched at lamina interfaces, and zero shear stress boundary conditions are enforced on the upper- and lower-most lamina surfaces. However, the through-thickness normal stress is assumed to be zero, and complete consistency between the strain-displacement equations for in-plane direct strain and transverse shear strain is not maintained. The CQUAD4 is thus seen to overcome the limitations of CLT for laminated plates, but does not represent all aspects of the kinematics of three-dimensional continua taking place in relatively thick laminates.

The CQUAD4 element is discussed in more depth in the following section.

THE CQUAD4 ELEMENT

The CQUAD4 is a four-noded planar element possessing membrane, flexural, and transverse shear stiffness. In the case of layered plates, individual laminae are not modeled explicitly; rather, equivalent stiffness matrices for the plate as a whole are defined. Each lamina is assumed to be in a state of plane stress, and the laminae are presumed to be perfectly bonded by infinitesimally thin non-shear-deformable layers. Each lamina is assumed to be specially orthotropic, with six independent elastic moduli when through-thickness direct stresses and strains are ignored. Any alignment of lamina fiber axis with respect to the local element coordinate system can be accomodated. Hence, any layup or stacking sequence can be handled (unidirectional, cross-ply, regular or irregular angle-ply). Layups unsymmetric with respect to plate midplane can also be modeled, as membrane-bending coupling is accounted for when it occurs. Each lamina may also be composed of a different orthotropic material, if desired.

The element's stiffness matrix terms for determining in-plane displacements and flexural rotations as a function of imposed forces and moments arise from CLT assumptions. The CQUAD4's force-versus strain equations for membrane, flexural, and membrane-flexure coupling (Ref. 4) are identical to those developed in sections 2.1 through 2.6 of Reference 6. The kinematic assumptions regarding in-plane and flexural strains and displacements follow classical assumptions and require no explanatory remarks here. Reference 4 documents the force-versus strain matrix terms for transverse shear strains. These are based on overall element equilibrium, continuity of transverse shear between adjacent laminae, and satisfaction of zero shear strain and stress boundary conditions on the upper- and lower-most laminate facings. As mentioned earlier, the strain-versus displacement matrix is based on the assumption that through-

thickness planar sections rotate with respect to the plate midsurface and also distort out of planes originally perpendicular to the midsurface.

The CQUAD4 is an isoparametric element, whose displacement fields are interpolated through space by linear variations of in-plane and transverse displacements (and rotations about midsurface) between grid points. The associated in-plane strains are constant between grid points but vary linearly with the thickness coordinate. However, transverse shear strain varies quadratically through each lamina thickness.

Those who use the CQUAD4 to model fiber-reinforced composite plates must realize that the input elastic moduli are effective moduli for a particular fiber-matrix combination. There are many different fibers in use (glass, carbon, kevlar, and boron are examples) and many resins or matrix materials, each of which has their own unique elastic moduli. Although matrix resins are usually considered to be isotropic, fibers have distinct extensional, transverse, and shear moduli. The effective in-plane moduli of an orthotropic continuum defined to be equivalent to the actual inhomogeneous fiber and resin system are (sometimes nonlinear) functions of the extensional, transverse, and shear moduli of the fiber, the extensional and shear moduli of the resin, and the Poisson's ratios of the fiber and resin. The fraction of the lamina volume occupied by fiber material is an important variable defining the magnitude of effective in-plane lamina moduli. Some strength-of-materials relationships defining effective lamina in-plane moduli as a function of constituent matrix and fiber moduli and fiber volume fraction are developed in sections 3.1 and 3.2 of reference 6. Reference 9 provides a handy tabulation of effective lamina elastic moduli under the assumption of a transversely isotropic lamina. Chamis provides formulas for effective out-of-plane shear moduli as well as the more commonly reported in-plane extension and shear moduli.

APPROACH

Specifics of the present vibration modeling study are now described.

PLATE VIBRATION SPECIMENS

It was desired that the validity of the CQUAD4 be proven by comparison to numerical results obtained independently by other researchers, and to experimental data, if possible. Lin, Ni, and Adams (Ref. 10,11) and Xiao, Lin, and Ju (Ref. 12) have published experimental data and finite element computations for the lowest six vibration modes of square CFRP and GFRP plates for free, unconstrained boundary conditions. They measured and computed both natural frequencies and damping loss factors, which makes their work almost uniquely complete and thorough. Reference 11 contains data for nine plates repeating that for four plates treated in reference 10. Reference 12 revisits three previously examined plates with a

more refined finite element formulation allowing plane sections to rotate and warp, with consistent correction of all strain-displacement relations for these kinematic conditions. This paper contains data for one additional new plate, making a total of ten unique plates in all (four CFRP and six GFRP). Refinement of their finite element method (Ref. 12) improved correlation of their predictions with measurements.

The geometric and material parameters of the ten plates studied by Lin et. al. and Xiao et. al. are listed (in SI units) in Table 1. The parameters given in reference 12 for plates 770 and 772 are inconsistent with those reported in reference 11. The NASTRAN study confirmed that the side lengths, thicknesses, average mass densities, and fiber volume fractions given for plates 770 and 772 in reference 11 are the correct values. Further correlation of plate parameters, frequencies, and mode shapes between references 10-12 revealed accidental reversal of mode shape plot labels in reference 11. In addition, two unidirectional GFRP plates of different size are reported in references 11 and 12 with the identification number 761. (They are herein distinguished from the other as 761L and 761X). These discrepancies initially caused much confusion, but the author is confident that the data in Table 1 is correct.

Some features of these plate specimens are notable. All of them are square, and have L/t ratios in the vicinity of 100 to 150. Even though such L/t would seem to be in the range of applicability of CLT, Xiao et. al. show that CLT, which totally ignores transverse shear deformations, overestimates natural frequencies by factors as high as sixteen percent over a theory with first-order shear correction. All of the laminates listed in Table 1 are symmetric about the plate midplane, eliminating flexure/extension coupling effects. Five plates (GFRP specimens 734, 761(L), 761(X) and CFRP specimens 762 and 764) have "specially orthotropic" lamina (all fibers aligned with the plate sides). For these plates, there is no coupling between in-plane extension and in-plane shearing, so their vibration mode shapes have nodal lines more or less parallel with the plate edges. The other five plates (765, 769, 771, 770, 772) have at least some plies with fibers angled relative to plate edges, providing more complex mode shapes.

All plates were tested with "free" edges (supported by soft foam rubber strips) and numerically analyzed with zero-constraint boundary conditions. (Although many practical design problems of interest would involve plate structures with boundary constraints, this feature eliminates uncertainties about which boundary degrees-of-freedom (DOF) to constrain to obtain "simply supported" edges). An iterative technique was used to obtain natural frequencies and modal damping loss factors. First, the specimens were excited into steady-state vibration by an electrodynamic shaker, and approximate resonance frequencies were determined. Nodal lines for each excited natural mode were located by the classical Chladni sand pattern technique. Then, for each mode of interest, locations of the support strips were then adjusted to align with nodal lines. A transient excitation technique was then used to obtain more precise

estimates of resonance frequencies and modal damping loss factors.

LAMINA MATERIAL PROPERTIES

Effective in-plane lamina elastic moduli are reported in Lin et. al. and Xiao et. al. These are listed in Table 2, in both SI and English units. These moduli pertain to a lamina microstructure where half of the total ply volume is occupied by fibers and half by the matrix. For each plate analyzed here, the moduli input to NASTRAN must be adjusted up or down from these nominal values, according to the measured fiber volume fraction (V_f) for each plate. In general, the moduli vary nonlinearly with V_f, but experimentally-verified semi-empirical equations are available for determining V_f-adjusted moduli. References 10-12 reported only the nominal moduli in Table 2, but provided a literature source (Ref. 13) for accomplishing the adjustments.

For orthotropic laminae in a state of plane stress (in the 1-2 plane), the only independent engineering moduli are E_{11}, E_{22}, G_{12}, and ν_{12}. The additional Poisson's ratio ν_{21} must satisfy the relationship:

$$\nu_{12} / E_{11} = \nu_{21} / E_{22}$$

The NASTRAN CQUAD4 element enforces this constraint on ν_{21} (Ref. 4). With these moduli, all in-plane strain and stress components are defined by the CLT. However, the NASTRAN CQUAD4 element also requires, as input, nonzero transverse shear moduli G_{13} and G_{23}, associated with out-of-plane shearing, which are not specified or required in CLT. Fortunately, fiber-reinforced lamina may often be assumed to be "transversely isotropic" in analysis of composite structures, as implied by reference 9. This means that if the lamina lies in the 1-2 plane, and the fibers are aligned in the 1-direction, then the transverse shear modulus G_{13} is equal to the in-plane shear modulus G_{12}. The transverse shear modulus associated with shearing of the matrix "around" the fibers and distortion of the fiber in a plane perpendicular to its axis (G_{23}) remains to be determined. To clarify these matters, the stress and strain components for a transversely isotropic lamina with zero direct stress normal to the lamina are illustrated in Figure 1.

Lin et. al. and Xiao et. al. did not report either of the transverse shear moduli used in their analyses. Educated guesses had to be made for both the CFRP and GFRP G_{23}. Reference 8 provides nondimensional elastic moduli for a CFRP-like material which are closely satisfied by the in-plane parameters for the CFRP in Table 2. According to reference 8, G_{23} should equal $0.2E_{22}$. This implied value of G_{23} was used in the present CFRP plate analyses, based on fiber volume fraction-adjusted E_{22}. For the glass fiber lamina, $G_{23} = 0.6G_{12}$ was assumed, based on in-house experience with such materials. The assumed out-of-plane moduli are indicated in the "notes" section of Table 2. G_{23} could also be estimated by methods reported in reference 9.

Table 3 contains lamina elastic moduli for each of the ten plates, after adjustment of the nominal moduli in Table 2 for fiber volume fraction. Lin et. al. did not correct the in-plane Poisson's ratio for fiber volume fraction, even though Ni and Adams show that it decreases appreciably for increasing V_f. Lin et. al. claim that accounting for this decrease had no significant effect on their calculated natural vibration frequencies. We match their assumption by keeping ν_{12} constant at 0.3 for all ten plates. In general, ν_{12} should be adjusted for V_f.

ASSUMPTIONS REGARDING LAMINATE BEHAVIOR

The kinematic assumptions of the CQUAD4 element have been discussed previously; namely, that planar sections perpendicular to the plate midplane can rotate and warp relative to the midplane. NASTRAN-computed natural frequencies for CQUAD4 plate idealizations will, subsequently, be compared to some CLT predictions (Ref. 12) and to the FEA predictions of Lin et. al. (Ref. 11) and Xiao et. al. (Ref. 12) These three approaches differ in accuracy, and it is important to understand how the NASTRAN predictions should compare with them. Kinematic assumptions are discussed first.

As discussed previously, CLT totally ignores any transverse shear deformation effect, and will always predict lower-order vibration frequencies which are too high for laminates with low L/t and high extensional-to-shear modulus ratios. In terms of through-thickness lamina kinematics, CLT prescribes linear variations of direct and in-plane shear strains, and zero transverse shear strains. The kinematic assumptions of Lin et. al. (Ref. 11) and within the CQUAD4 (Ref. 4) are identical, and imply linear through-thickness variations of direct and in-plane shear strains and quadratic through-thickness variations of transverse shear strains, with zero shear stress boundary conditions on the upper- and lowermost lamina facings satisfied. However, this thick plate-type theory is only an approximation; consistent correction of <u>all</u> strain-displacement relationships when cross-section warping is allowed requires <u>cubic</u> through-thickness variations of direct and in-plane shear strains. Xiao et. al. (Ref. 12) include this considerable complication in their plate-type FEA formulation, which can be understood as a special case of three-dimensional elasticity.

From an understanding of kinematic assumptions alone, CQUAD4 composite plate idealizations should provide natural frequency estimates that are (1), more accurate than CLT, (2) as accurate as the Lin et. al. predictions, and (3) less accurate than the Xiao et. al. predictions. However, other factors will influence the comparisons between FEA-predicted frequencies; particularly, the polynomial form of the interpolation functions expressing element displacement fields in terms of grid point displacements, and the mass matrix formulation (consistent or lumped). The CQUAD4 utilizes linear interpolation functions with respect to the element's four grid points. Lin et. al. do not specify the interpolation func-

tions used in their "8-node 40-degree-of-freedom" elements, although they can be guessed to be of at least quadratic order.

NASTRAN ANALYSES

The results of the NASTRAN computations are now compared to the calculations and experimental data in references 10-12.

FEATURES OF THE NASTRAN PLATE IDEALIZATIONS

Lin et. al. and Xiao et. al. employed a 6-by-6 mesh of 8-noded isoparametric rectangular elements in all of their plate FEA idealizations. Each element possessed 40 DOF, (5 per grid point), implying that all rotations about axes normal to the plate surface were constrained. As in the CQUAD4, they applied a numerical conditioning factor to transverse shear stiffness terms to eliminate excessive shear stiffness ("shear locking"); a consequence of numerical integration of element stiffness. The NASTRAN CQUAD4 elements also have five DOF per node, with normal axis rotation constraints applied, and are also conditioned to avoid shear locking.

The CQUAD4 differs from the Lin and Xiao et. al. elements in one important way; they are 4-noded isoparametric quadrilaterals and thus have linear interpolation of in-plane displacements between grid points instead of quadratic interpolation. Thus, although the Lin et. al. element is kinematically similar to the CQUAD4 as far as through-thickness shear effects are concerned, the elements' assumed in-plane displacement fields differ as a function of the plate's in-plane dimensions. The Xiao et. al. element provides for a more complex through-thickness displacement and strain distribution than the Lin et. al. element and the CQUAD4, as discussed earlier.

The NASTRAN CQUAD4 meshes used here consist of a 12-by-12 grid of elements, with 169 grid points and 845 unconstrained DOF. These idealizations are roughly comparable to the Lin and Xiao models in modal displacement field interpolation quality. Three of the plates were initially modeled with 6-by-6 meshes with 49 grid points and 245 DOF, but these idealizations did not provide sufficient mode shape resolution to be acceptable. The Lin and Xiao et. al. mesh is compared to the NASTRAN mesh in Figure 2.

The edges of the NASTRAN plate idealizations were unconstrained, and all rotations about axes normal to the plate surface were suppressed. A SUPORT input record imposing fictitious constraints on all five remaining DOF on one grid point was used to provide zero-frequency rigid body modes. The FEER eigenmode extraction method was used in NASTRAN Rigid Format 3 (normal modes analysis), with the lowest twenty modes requested. The Inverse Power method was employed in some trial runs; it provided about half as many frequencies as FEER but at more than two times greater run time and cost. All computations were performed by RPK COSMIC NASTRAN, 1990 release, installed on the DTRC CRAY X-MP supercomputer in a COS operating system environment. Typically, 22 to 24 modes were extracted by FEER in 23 to 24 CP seconds.

Lin and Xiao do not mention whether they used lumped or consistent mass matrix formulations. Both options were considered in the NASTRAN study.

NASTRAN MODAL ANALYSIS RESULTS

Initial NASTRAN analyses utilized nominal elastic moduli based on fifty percent fiber volume fraction. Although predicted frequencies were in the general vicinity of measured values, they did not compare with CLT results, the Lin et. al. results, or the Xiao et. al. results in the expected way. That is, the CQUAD4 did not necessarily appear more accurate than CLT and less accurate than the Xiao et. al. approach. It suffices to say that fiber volume fraction strongly influences effective moduli and must be accounted for to obtain credible composite plate modal predictions.

Relative NASTRAN frequency predictions are compared with CLT, Lin's, and Xiao's results in Table 4. There is, in general, good correlation with measurements, and NASTRAN's frequency error trends are comparable to those in the Lin et. al. analyses (especially those for a consistent mass matrix). The fact that effective lamina elastic moduli must be corrected for fiber volume fraction to obtain credible natural frequency predictions for laminated composite plates is emphasized in Table 5, where root-mean-square (RMS) values of frequency prediction percentage error are tabulated for the six modes of each plate. RMS error is seen to be significantly reduced in most cases when fiber volume fraction-corrected lamina moduli are employed. The major exception is plate 765, which still suffers from some large unknown systematic error making predicted frequencies far too low. Results for plate 770 were not much changed since actual V_f was already close to one-half. RMS errors for plates 764 and 771 remain at ten percent and above. However, the major part of these high errors involves their fundamental modes, which can be easily impacted by test article boundary constraint. (The Lin et. al. analysis also predicted overly high frequencies for these modes).

Absolute measured and predicted natural frequencies are summarized in Table 6, which lists Lin et. al. measurements and computations and the NASTRAN CQUAD4 idealization results for lumped and consistent mass. Mode-by-mode and average percentage frequency prediction errors are listed in Table 7 along with mode shape descriptions. The NASTRAN lumped mass model gives the lowest average error in seven of ten cases, and the NASTRAN consistent mass model is best in two of the three remaining cases. (Interestingly, the consistent mass model errors roughly parallel those of the Lin model). Lin et. al. calculations are "best" only for plate 765, for which the author believes a parameter was misdocumented in reference 11. In six of the nine plates other than 765, NASTRAN predicts frequencies that are all at or within ten percent of measured. In the other three, errors are greater than ten percent only for the first and/or second modes, and these roughly parallel the errors in the Lin et. al. analyses.

Plots of chosen NASTRAN-computed eigenmodes are presented in Figures 3-8. Plate 761X does not appear since its mode shapes are identical to plate 761L, and plates 764, 770, and 772 are omitted since their mode shapes are very similar to those of plates 734, 769, and 771. The nodal patterns can be confirmed as being identical to those measured. (Figures 3-8 should be compared to Tables 8, 7, 10, 9, 11, and 3, respectively, of reference 11). Finer details of some NASTRAN modes, particularly the veering of nodal lines away from each other in plates with angled plies, are more easily seen in colored graphics terminal displays. Only the plates with specially orthotropic ply layups (734, 761L, 761X, 762, 764) exhibit eigenmodes with nodal lines more or less parallel to the plate sides. Most of these modes are essentially beam-like flexural modes with or without phase changes at one symmetry plane. In contrast, plates with angled plies possess a larger number of more complex plate flexural modes.

The natural frequency results obtained via NASTRAN CQUAD4 plate element idealizations in these simple composite plate vibration problems are judged to be acceptably accurate for engineering purposes. The element performs as well as alternative formulations of similar accuracy (the Lin et. al. element) for both GFRP and highly anisotropic CFRP plates for a variety of ply geometries. Potential users of the element must be cautioned that this validation effort concerned plates with L/t ratios in the vicinity of 100 to 150. For such L/t, modeling of laminate transverse shear stiffness helps to eke out a few percent in low-order natural frequency accuracy, but is not absolutely essential to obtain rough-cut results. A more critical test of the CQUAD4 for modeling highly anisotropic laminates would have to concern plates with L/t lower than, say, about 50.

It should be mentioned that Lin et. al. and Xiao et. al. also measured and computed the specific damping capacities (2π times the modal loss factor) of each mode. Their FEA program was capable of modeling orthotropic lamina damping properties. No attempt was made to predict modal damping factors in this effort, as NASTRAN is currently restricted to the modeling of isotropic material damping.

SUMMARY

The performance of the NASTRAN CQUAD4 membrane and plate element in analysis of undamped natural vibration modes of thin fiber-reinforced composite plates has been evaluated. The element provides natural frequency estimates that are comparable in accuracy to alternative formulations, and, in most cases, deviate by less than ten percent from experimentally measured frequencies. The predictions lie within roughly equal accuracy bounds for the two material types treated (GFRP and CFRP), and for the ply layups considered (unidirectional, cross-ply, angle-ply). Effective elastic lamina moduli had to be adjusted for measured fiber volume fraction to attain this level of accuracy; nominal moduli at fifty percent volume fraction gave significantly inferior frequency estimates. The lumped mass option provided more accurate frequen-

cies than the consistent mass option.

This evaluation concerned only plates with L/t ratios on the order of 100 to 150. Since the CQUAD4 utilizes first-order corrections for transverse laminate shear stiffness, the element should provide useful frequency estimates for plate-like structures with lower L/t. For plates with L/t below 20, consideration should be given to idealizing with 3-D solid elements.

Based on the observation that natural frequencies and mode shapes are predicted with acceptable engineering accuracy, it is concluded that the CQUAD4 should be a useful and accurate element for transient shock and steady-state vibration analysis of Naval ship structures.

REFERENCES

1. Everstine, G. C. and M. S. Marcus, "Finite Element Prediction of Loss Factors for Structures with Frequency-Dependent Damping Treatments", 13th NASTRAN User's Colloquium, NASA CP-2373, National Aeronautics and Space Administration, Washington, D. C., pp. 419-430 (May 1985).

2. Everstine, G. C., F. M. Henderson, E. A. Schroeder, R. R. Lipman, "A General Low Frequency Acoustic Radiation Capability for NASTRAN", 14th NASTRAN User's Colloquium, NASA CP-2419, National Aeronautics and Space Administration, Washington, D. C., pp. 293-310 (May 1986).

3. Everstine, G. C. and A. J. Quezon, "User's Guide to the Coupled NASTRAN/ Helmholtz Equation Capability (NASHUA) for Acoustic Radiation and Scattering", Third Edition, DTRC CMLD-88/03 (Feb 1988).

4. Venkayya, V. B., "CQUAD4 Seminar," Presentation given at 16th NASTRAN User's Colloquium (Apr 1988).

5. Marcus, M. S., G. C. Everstine, M. M. Hurwitz, "Experiences with the QUAD4 Element for Shell Vibrations", 16th NASTRAN User's Colloquium, NASA CP-2505, pp. 39-43 (Apr 1988).

6. Jones, R. M. Mechanics of Composite Materials, Hemisphere Publishing Corporation, New York, New York, 1975.

7. Cremer, L., M. Heckl, E. Ungar, Structure-Borne Sound, Springer-Verlag, New York, New York, 1973.

8. Mallikarjuna and T. Kant, "Free Vibration of Symmetrically Laminated Plates using a Higher-Order Theory with Finite Element Technique", Int. J. Num. Meth. Eng., Vol. 28, pp. 1875-1889 (1989).

9. Chamis, C. C., "Simplified Composite Micromechanics Equations for Hygral, Thermal, and Mechanical Properties", SAMPE Quarterly, Vol. 15, No. 3, pp. 14-23 (Apr 1984).

10. Adams, R. D., D. X. Lin, R. G. Ni, "Prediction and Measurement of the Natural Frequencies and Damping Capacity of Carbon Fiber-Reinforced Plastic Plates", Journal de Physique, Colloque No. 9, pp. C9-525 - C9-530 (1983).

11. Lin, D. X., R. G. Ni, R. D. Adams, "Prediction and Measurement of the Vibrational Damping Parameters of Carbon and Glass Fibre-Reinforced Plastic Plates", J. Composite Materials, Vol. 18, pp. 132-152 (Mar 1984).

12. Xiao, C. Z., D. X. Lin, F. Ju, "Finite Element Analysis on Modal Parameters of Anisotropic Laminated Plates", ASME J. Vib. Acous. Stress and Reliability in Design, Vol. 110, pp. 473-477 (Oct 1988).

13. Ni, R. G. and R. D. Adams, "A Rational Method for Obtaining the Dynamic Mechanical Properties of Laminae for Predicting the Stiffness and Damping of Laminated Plates and Beams", Composites, Vol. 15, No. 3, pp. 193-199 (Jul 1984).

Table 1. Geometric and material parameters of ten fiber-reinforced plastic plates tested and analyzed by Lin et. al. and Xiao et. al.

Plate Ident. Number	Plate Material	Plate Length L (mm)	Plate Thickness t (mm)	Fiber Volume Fraction V_f	Mass Density ρ (kg/m^3)	Number of Plies	Ply Layup (degrees; see Figure 2)	Source of Data (ref. no.)
734	GFRP	227.0	2.05	0.451	1813.9	8	[0/90/0/90]	10,11,12
761L	GFRP	182.75	1.64	0.568	1971.0	8	[0]	11
761X	GFRP	249.0	2.28	0.530	1924.7	8	[0]	12
765	GFRP	230.5	1.45	0.607	2023.6	8	[45/-45/45/-45]	11
769	GFRP	224.2	1.37	0.621	2041.7	8	[0/90/45/-45]	11
771	GFRP	204.6	2.11	0.592	2003.5	12	$[(0/-60/60)_2]$	10,11
762	CFRP	178.0	1.58	0.516	1566.0	8	[0]	11
764	CFRP	234.5	2.12	0.342	1446.2	8	[0/90/0/90]	10,11
770	CFRP	215.0	1.62	0.494	1551.4	8	[0/90/45/-45]	11,12
772	CFRP	215.6	2.02	0.618	1636.4	12	$[(0/-60/60)_2]$	10,11,12

NOTE: All laminates are symmetric about plate midplane.

Table 2. Nominal in-plane effective elastic moduli of GFRP and CFRP laminae at fifty percent fiber volume fraction

Material	Fiber type	Resin type	E_{11} (Gpa)	E_{11} ($psi/10^6$)	E_{22} (GPa)	E_{22} ($psi/10^6$)	G_{12} (GPa)	G_{12} ($psi/10^6$)	ν_{12}
GFRP	"Glass"	DX210 epoxy	37.78	5.48	10.90	1.58	4.91	0.71	0.3
CFRP	HM-S	DX210 epoxy	172.7	25.0	7.20	1.04	3.76	0.55	0.3
DX210 epoxy	-----	-----	3.21	0.47	3.21	0.47	1.20	0.17	0.34

NOTE: $G_{23} = 0.6(G_{12}) = 2.94$ GPa is assumed for GFRP,
$G_{23} = 0.2(E_{22}) = 1.44$ GPa is assumed for CFRP.

Table 3. In-plane and out-of-plane effective elastic moduli for GFRP and CFRP laminae, adjusted for fiber volume fraction of each plate

Plate Ident. Number	Plate Material	Fiber Volume Fraction V_f	E_{11} (GPa)	E_{22}, E_{33} (GPa)	G_{12}, G_{13} (GPa)	G_{23} (GPa)
734	GFRP	0.451	34.4	9.7	4.3	2.6
761L	GFRP	0.568	42.5	13.0	5.7	3.4
761X	GFRP	0.530	39.9	12.0	5.2	3.1
765	GFRP	0.607	45.2	14.2	6.5	3.9
769	GFRP	0.621	46.2	14.4	6.7	4.0
771	GFRP	0.592	44.1	14.0	6.2	3.7
762	CFRP	0.516	178.0	7.4	3.9	1.5
764	CFRP	0.342	119.0	5.6	2.6	1.1
770	CFRP	0.494	171.0	7.1	3.7	1.4
772	CFRP	0.618	213.0	8.7	5.0	1.7

NOTE: ν_{12} = 0.30 is assumed for all laminates, with no V_f adjustment.

Table 4. Comparison of natural frequencies from final NASTRAN CQUAD4 idealizations and predictions of Lin and Xiao et. al. to measured data

Plate Number and params.	Mode Number	Natural Frequency Ratios, (computed / measured)				
		CLT ref. 12	Lin et. al. ref. 11,12	Xiao et. al. ref. 12	NASTRAN 12-by-12 lumped	NASTRAN 12-by-12 consis.
734 GFRP 8 plies [0/90/0/90]sym L/t = 110.7	1	1.20	1.07	0.98	1.03	1.05
	2	1.09	1.00	1.00	0.94	0.97
	3	1.20	1.03	1.00	0.98	1.01
	4	1.11	1.05	1.03	0.99	1.03
	5	1.12	1.04	1.01	1.00	1.03
	6	1.11	1.06	1.01	0.98	1.04

Table 4. (Continued)

Plate Number and params.	Mode Number	Natural Frequency Ratios, (computed / measured)				
		CLT ref. 12	Lin et. al. ref. 11	Xiao et. al. ref. 12	NASTRAN 12-by-12 lumped	NASTRAN 12-by-12 consis.
761L GFRP 8 plies [0] sym L/t = 111.4	1	----	1.13	----	1.11	1.13
	2	----	1.00	----	0.97	1.00
	3	----	1.05	----	1.02	1.05
	4	----	1.00	----	0.94	0.97
	5	----	1.04	----	0.99	1.02
	6	----	1.03	----	0.97	1.03
761X GFRP 8 plies [0] sym L/t = 109.2	1	1.18	1.09	0.98	1.10	1.11
	2	1.20	1.08	1.00	1.02	1.05
	3	1.20	1.08	0.98	1.05	1.08
	4	1.08	0.99	0.99	0.94	0.96
	5	1.10	1.02	0.99	0.98	1.02
	6	1.14	1.03	0.99	0.95	1.01
765 GFRP 8 plies [45/-45/ 45/-45] sym L/t = 159.0	1	----	1.09	----	0.82	0.83
	2	----	0.88	----	0.65	0.67
	3	----	0.95	----	0.68	0.70
	4	----	1.07	----	0.78	0.81
	5	----	1.06	----	0.78	0.81
	6	----	1.02	----	0.72	0.77

Table 4. (Continued)

Plate Number and params.	Mode Number	Natural Frequency Ratios, (computed / measured)				
		CLT ref. 12	Lin et. al. ref.11	Xiao et. al. ref. 12	NASTRAN 12-by-12 lumped	NASTRAN 12-by-12 consis.
769 GFRP 8 plies [0/90/45/-45]sym L/t = 163.6	1	----	0.95	----	0.93	0.95
	2	----	1.08	----	1.03	1.06
	3	----	0.98	----	0.92	0.94
	4	----	1.01	----	0.96	0.99
	5	----	1.04	----	0.99	1.03
	6	----	1.01	----	0.94	0.99
771 GFRP 12 plies [0/-60/60/0/-60/60] sym L/t = 97.0	1	----	1.20	----	1.19	1.20
	2	----	1.17	----	1.13	1.16
	3	----	0.98	----	0.93	0.96
	4	----	1.06	----	1.02	1.06
	5	----	1.07	----	1.03	1.07
	6	----	1.03	----	0.95	1.01
762 CFRP 8 plies [0] sym L/t = 112.7	1	----	1.03	----	1.01	1.02
	2	----	1.10	----	1.02	1.05
	3	----	1.06	----	0.99	1.04
	4	----	1.11	----	1.01	1.08
	5	----	1.10	----	1.00	1.07
	6	----	1.03	----	1.00	1.03

Table 4. (Continued)

Plate Number and params.	Mode Number	Natural Frequency Ratios, (computed / measured)				
		CLT ref. 12	Lin et. al. ref. 11	Xiao et. al. ref. 12	NASTRAN 12-by-12 lumped	NASTRAN 12-by-12 consis.
764 CFRP 8 plies [0/90/0/90] sym L/t = 110.6	1	----	0.84	----	0.81	0.82
	2	----	0.97	----	0.95	0.97
	3	----	0.97	----	0.93	0.96
	4	----	0.99	----	0.97	0.99
	5	----	1.00	----	0.97	1.00
	6	----	0.98	----	0.92	0.97
770 CFRP 8 plies [0/90/45/-45]sym L/t = 132.7	1	1.14	1.11	1.08	1.10	1.12
	2	1.16	1.11	1.06	1.09	1.12
	3	1.15	1.09	1.00	1.06	1.10
	4	1.07	1.00	1.00	0.98	1.01
	5	1.15	1.08	0.99	1.06	1.09
	6	1.11	1.03	1.00	0.99	1.04
772 CFRP 12 plies [0/-60/60/0/-60/60] sym L/t = 106.7	1	1.07	1.05	1.00	1.04	1.05
	2	1.05	1.03	1.00	0.99	1.02
	3	1.07	1.04	1.01	1.01	1.04
	4	1.10	1.06	1.00	1.02	1.06
	5	1.09	1.05	1.00	1.02	1.05
	6	1.09	1.03	0.99	0.97	1.03

Table 5. Root-mean-square errors in NASTRAN-computed natural frequencies for ten composite plates for uncorrected and corrected effective lamina elastic moduli

Plate Number	RMS error in NASTRAN-predicted frequency	
	With uncorrected moduli (percent)	With corrected moduli (percent)
734	5.3	2.9
761L	8.8	5.5
761X	10.7	5.7
765	34.4	26.7
769	15.6	5.4
771	9.7	10.1
762	2.1	0.8
764	11.9	9.6
770	7.1	6.6
772	9.6	2.5

Table 6. Comparison of absolute measured and predicted composite plate natural frequencies of Lin et. al. with NASTRAN CQUAD4 computations

Plate Number and params.	Mode Number	Natural Frequencies (Hz)			
		Lin et. al., ref. 10-12		NASTRAN 12-by-12	NASTRAN 12-by-12
		measured	computed	lumped	consis.
734 GFRP 8 plies [0/90/0/90]sym L/t = 110.7	1	62.2	66.4	64.2	65.0
	2	131.4	131.6	123.8	127.4
	3	159.2	164.5	156.4	160.9
	4	180.5	189.8	177.9	184.0
	5	200.1	208.9	199.2	206.0
	6	326.7	347.2	321.2	338.4

Table 6. (Continued)

Plate Number and params.	Mode Number	Natural Frequencies (Hz)			
		Lin et. al., ref. 10-12 measured	Lin et. al., ref. 10-12 computed	NASTRAN 12-by-12 lumped	NASTRAN 12-by-12 consis.
761L GFRP 8 plies [0] sym L/t = 111.4	1	78.1	88.1	86.9	88.0
	2	131.2	130.7	127.1	130.7
	3	211.5	222.2	215.0	222.2
	4	246.0	246.1	232.1	238.7
	5	287.1	297.8	284.1	294.2
	6	362.6	374.4	352.9	375.0
761X GFRP 8 plies [0] sym L/t = 109.2	1	57.2	62.5	62.9	63.7
	2	90.3	97.4	92.5	95.2
	3	148.7	160.5	155.9	161.2
	4	181.6	180.2	170.4	175.2
	5	211.2	215.9	207.5	214.9
	6	270.5	278.8	256.9	272.9
765 GFRP 8 plies [45/-45/ 45/-45] sym L/t = 159.0	1	84.0	91.3	68.7	69.6
	2	114.0	99.9	74.4	76.6
	3	157.0	149.5	107.1	110.0
	4	199.3	212.6	156.3	161.6
	5	213.4	226.7	167.2	173.4
	6	346.6	353.5	249.6	265.5

Table 6. (Continued)

Plate Number and params.	Mode Number	Natural Frequencies (Hz)			
		Lin et. al., ref. 10-12 measured	Lin et. al., ref. 10-12 computed	NASTRAN 12-by-12 lumped	NASTRAN 12-by-12 consis.
769 GFRP 8 plies [0/90/45/-45]sym L/t = 163.6	1	58.2	55.5	54.4	55.1
	2	91.6	99.0	94.5	97.2
	3	125.5	123.0	115.2	118.4
	4	150.4	151.3	143.8	148.7
	5	156.8	163.0	155.7	161.1
	6	277.3	279.4	260.5	274.4
771 GFRP 12 plies [0/-60/60/0/-60/60] sym L/t = 97.0	1	90.4	108.2	107.4	108.8
	2	144.7	168.6	163.6	168.4
	3	222.3	218.6	206.6	212.4
	4	264.1	280.2	270.6	279.8
	5	281.1	301.0	290.9	300.9
	6	492.6	505.2	469.7	499.3
762 CFRP 8 plies [0] sym L/t = 112.7	1	81.5	83.6	82.2	83.3
	2	107.4	118.4	109.4	112.5
	3	196.6	207.8	198.4	205.1
	4	295.5	329.4	299.2	318.2
	5	382.5	419.8	383.6	410.2
	6	531.0	546.9	530.6	545.9

Table 6. (Continued)

Plate Number and params.	Mode Number	Natural Frequencies (Hz)			
		Lin et. al., ref. 10-12		NASTRAN 12-by-12	NASTRAN 12-by-12
		measured	computed	lumped	consis.
764 CFRP 8 plies [0/90/0/90] sym L/t = 110.6	1	68.9	58.1	55.5	56.2
	2	218.9	213.3	206.9	212.8
	3	251.2	243.5	233.3	241.5
	4	305.4	302.5	294.9	303.4
	5	323.5	324.2	312.7	323.7
	6	452.5	441.6	414.5	437.8
770 CFRP 8 plies [0/90/45/-45]sym L/t = 132.7	1	77.8	86.3	85.9	87.0
	2	202.7	224.5	220.6	226.9
	3	258.0	280.4	273.9	283.4
	4	298.7	298.8	293.6	302.0
	5	322.0	348.4	340.6	352.4
	6	496.7	512.2	490.0	517.3
772 CFRP 12 plies [0/-60/60/0/-60/60] sym L/t = 106.7	1	156.6	165.2	162.7	165.0
	2	272.0	279.1	269.9	277.6
	3	372.3	387.8	376.9	387.6
	4	407.8	432.6	416.7	431.1
	5	486.1	511.4	494.7	512.0
	6	779.0	800.4	752.6	799.4

Table 7. Mode-by-mode tabulation of NASTRAN CQUAD4 idealization frequency prediction errors, with averaged percentage errors and eigenmode descriptions

Plate Number and params.	Mode Number	Percentage errors			Eigenmode description
		Lin et. al.	NASTRAN 12-by-12 lumped	NASTRAN 12-by-12 consis.	
734 GFRP 8 plies [0/90/0/90]sym L/t = 110.7	1	+ 7	+ 3	+ 5	shear and flexure
	2	0	- 6	- 3	2-noded beam abt. weak axis
	3	+ 3	- 2	+ 1	2-noded beam abt. strong axis
	4	+ 5	- 1	+ 3	2-noded beam abt. weak axis + shear
	5	+ 4	0	+ 3	2-noded beam abt. strong axis + shear
	6	+ 6	- 2	+ 4	fundamental plate flexure
	avg.	+ 4.2	- 1.3	+ 2.2	
761L GFRP 8 plies [0] sym L/t = 111.4	1	+ 13	+ 11	+ 13	shear and flexure
	2	0	- 3	0	2-noded beam abt. weak axis
	3	+ 5	+ 2	+ 5	2-noded beam abt. weak axis + shear
	4	0	- 6	- 3	2-noded beam abt. strong axis
	5	+ 4	- 1	+ 2	2-noded beam abt. strong axis + shear
	6	+ 3	- 3	+ 3	3-noded beam abt. weak axis
	avg.	+ 4.2	0	+ 3.3	
761X GFRP 8 plies [0] sym L/t = 109.2	1	+ 9	+ 10	+ 11	shear and flexure
	2	+ 8	+ 2	+ 5	2-noded beam abt. weak axis
	3	+ 8	+ 5	+ 8	2-noded beam abt. weak axis + shear
	4	- 1	- 6	- 4	2-noded beam abt. strong axis
	5	+ 2	- 2	+ 2	2-noded beam abt. strong axis + shear
	6	+ 3	- 5	+ 1	3-noded beam abt. weak axis
	avg.	+ 4.8	+ 0.7	+ 3.8	

Table 7. (Continued)

Plate Number and params.	Mode Number	Percentage errors			Eigenmode description
		Lin et. al.	NASTRAN 12-by-12 lumped	NASTRAN 12-by-12 consis.	
765 GFRP 8 plies [45/-45/ 45/-45] sym L/t = 159.0	1	+ 9	- 18	- 17	plate flexural
	2	- 12	- 35	- 33	plate flexural
	3	- 5	- 32	- 30	plate flexural
	4	+ 7	- 22	- 19	plate flexural
	5	+ 6	- 22	- 19	plate flexural
	6	+ 2	- 28	- 23	plate flexural
	avg.	+ 1.2	- 26.2	- 23.5	
769 GFRP 8 plies [0/90/45/ -45]sym L/t = 163.6	1	- 5	- 7	- 5	shear and flexure
	2	+ 8	+ 3	+ 6	2-noded beam abt. weak axis
	3	- 2	- 8	- 6	2-noded beam abt. strong axis
	4	+ 1	- 4	- 1	plate flexural
	5	+ 4	- 1	+ 3	plate flexural
	6	+ 1	- 6	- 1	plate flexural
	avg.	+ 1.2	- 3.8	- 0.7	
771 GFRP 12 plies [0/-60/60 /0/-60/60] sym L/t = 97.0	1	+ 20	+ 19	+ 20	shear and flexure
	2	+ 17	+ 13	+ 16	2-noded beam abt. weak axis
	3	- 2	- 7	- 4	2-noded beam abt. strong axis
	4	+ 6	+ 2	+ 6	plate flexural
	5	+ 7	+ 3	+ 7	plate flexural
	6	+ 3	- 5	+ 1	3-noded beam abt. weak axis
	avg.	+ 8.5	+ 4.2	+ 7.7	

Table 7. (Continued)

Plate Number and params.	Mode Number	Percentage errors			Eigenmode description
		Lin et. al.	NASTRAN 12-by-12 lumped	NASTRAN 12-by-12 consis.	
762 CFRP 8 plies [0] sym L/t = 112.7	1	+ 3	+ 1	+ 2	shear and flexure
	2	+ 10	+ 2	+ 5	2-noded beam abt. weak axis
	3	+ 6	- 1	+ 4	2-noded beam abt. weak axis + shear
	4	+ 11	+ 1	+ 8	3-noded beam abt. weak axis
	5	+ 10	0	+ 7	3-noded beam abt. weak axis + shear
	6	+ 3	0	+ 3	2-noded beam abt. strong axis
	avg.	+ 7.2	+ 0.5	+ 4.8	
764 CFRP 8 plies [0/90/0/90] sym L/t = 110.6	1	- 16	- 19	- 18	shear and flexure
	2	- 3	- 5	- 3	2-noded beam abt. weak axis
	3	- 3	- 7	- 4	2-noded beam abt. weak axis + shear
	4	- 1	- 3	- 1	2-noded beam abt. strong axis
	5	0	- 3	0	2-noded beam abt. strong axis + shear
	6	- 2	- 8	- 3	fundamental plate flexure
	avg.	- 4.2	- 7.5	- 4.8	
770 CFRP 8 plies [0/90/45/-45]sym L/t = 132.7	1	+ 11	+ 10	+ 12	shear and flexure
	2	+ 11	+ 9	+ 12	2-noded beam abt. weak axis
	3	+ 9	+ 6	+ 10	plate flexural
	4	0	- 2	+ 1	2-noded beam abt. strong axis
	5	+ 8	+ 6	+ 9	plate flexural
	6	+ 3	- 1	+ 4	plate flexural
	avg.	+ 7.0	+ 4.7	+ 8.0	

Table 7. (Continued)

Plate Number and params.	Mode Number	Percentage errors			Eigenmode description
		Lin et. al.	NASTRAN 12-by-12 lumped	NASTRAN 12-by-12 consis.	
772 CFRP 12 plies [0/-60/60 /0/-60/60] sym L/t = 106.7	1	+ 5	+ 4	+ 5	shear and flexure
	2	+ 3	- 1	+ 2	2-noded beam abt. weak axis
	3	+ 4	+ 1	+ 4	2-noded beam abt. strong axis
	4	+ 6	+ 2	+ 6	plate flexural
	5	+ 5	+ 2	+ 5	plate flexural
	6	+ 3	- 3	+ 3	3-noded beam abt. weak axis
	avg.	+ 4.3	+ 0.8	+ 4.2	

ASSUMPTIONS

(1). Plane stress ($\sigma_3 = 0$), but nonzero transverse shear strains

(2). $\nu_{21} = \nu_{12}(E_2/E_1)$

(3). 2-3 plane is plane of transverse isotropy, hence $G_{13} = G_{12}$

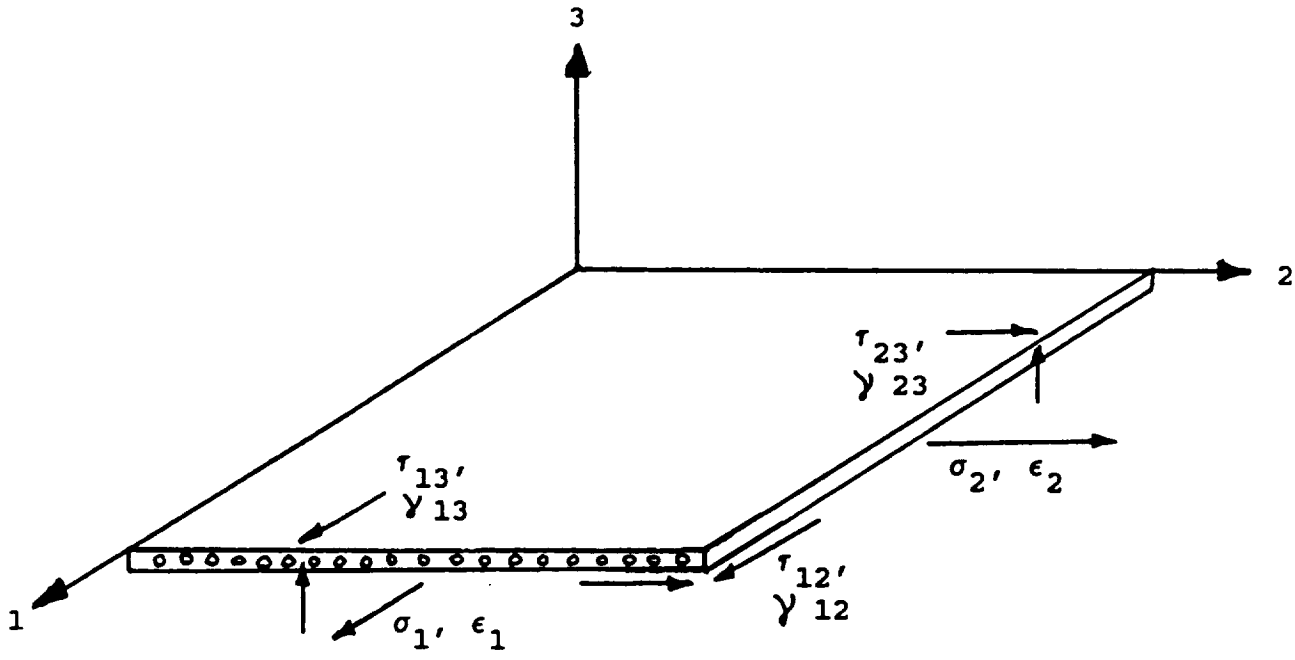

Figure 1. Stress and strain components for a fiber-reinforced lamina

Notes: Positive X-axis: fiber orientation angle of 0 degrees
Positive Y-axis: fiber orientation angle of 90 degrees

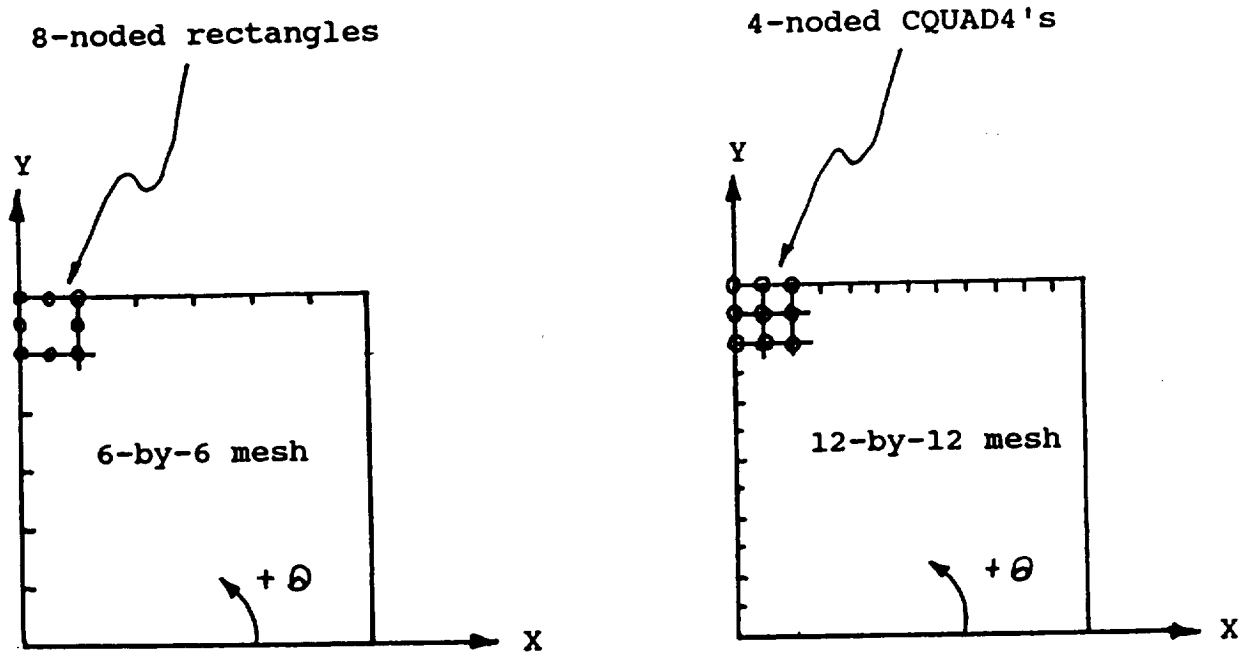

(i) Lin and Xiao et. al. idealization

(ii) NASTRAN CQUAD4 idealization

Figure 2. Plate element meshes used by Lin and Xiao et. al. and in NASTRAN analyses

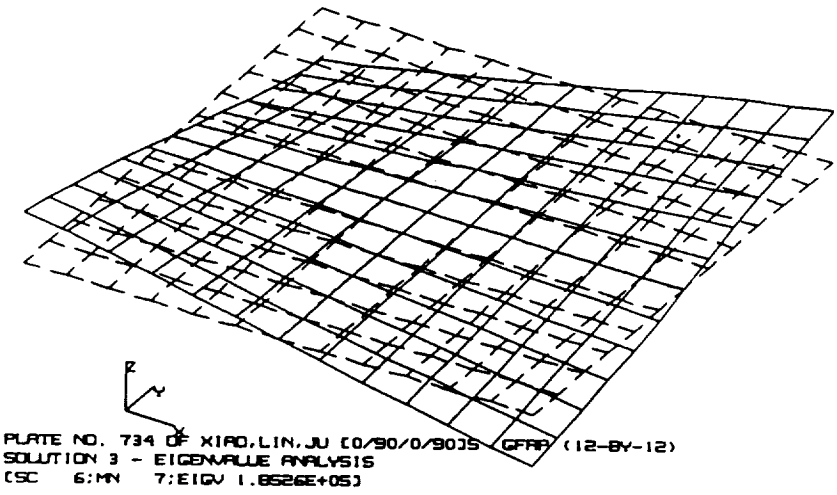

Fig. 3a. Plate 734, Mode 1

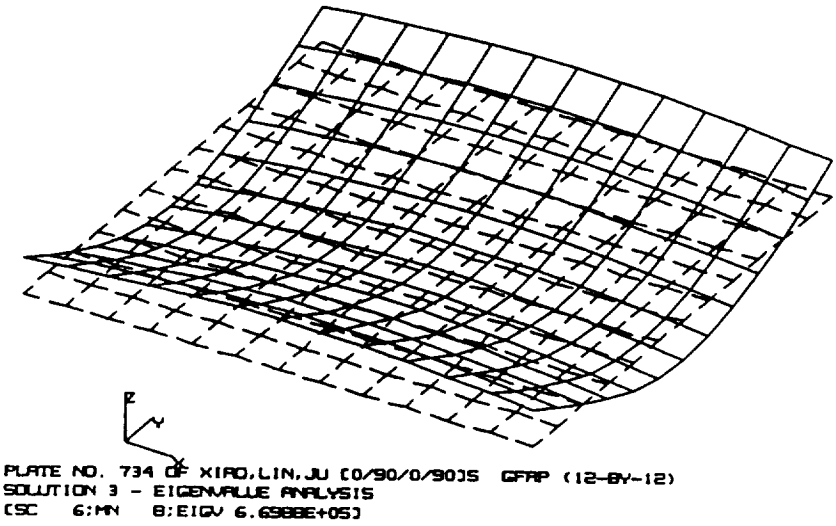

Fig 3b. Plate 734, Mode 2

Figure 3. NASTRAN-computed eigenmodes for plate 734

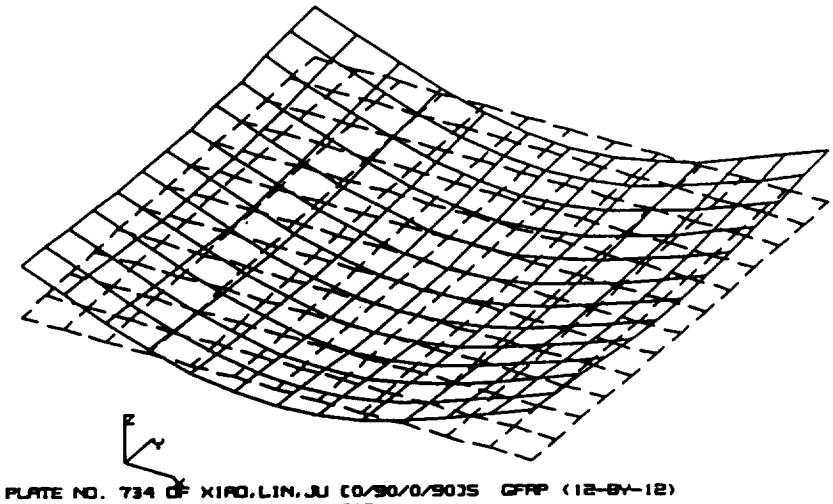

Fig. 3c. Plate 734, Mode 3

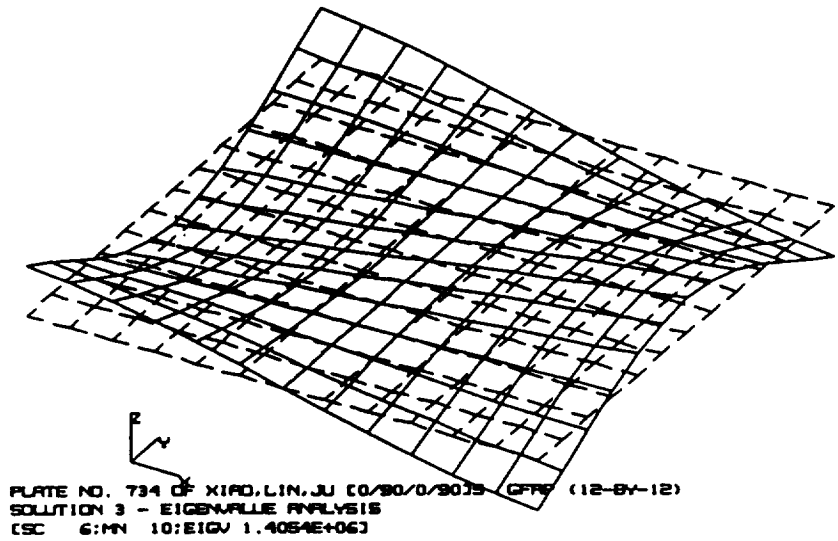

Fig. 3d. Plate 734, Mode 4

Figure 3. (Continued)

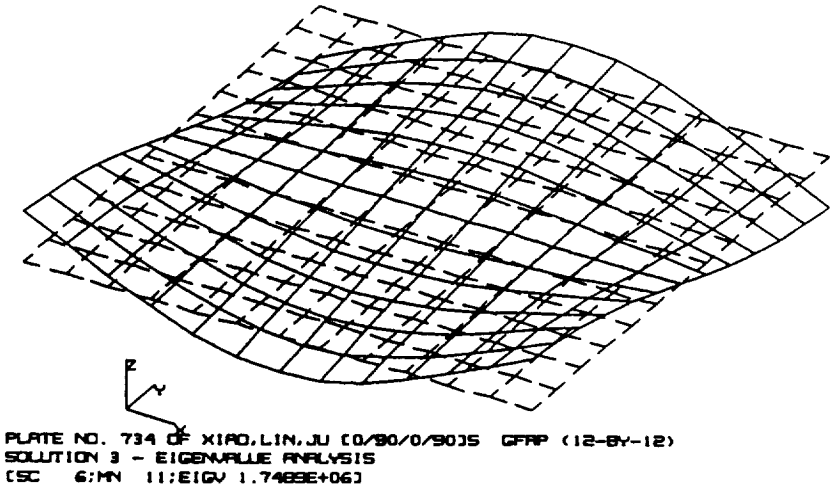

Fig. 3e. Plate 734, Mode 5

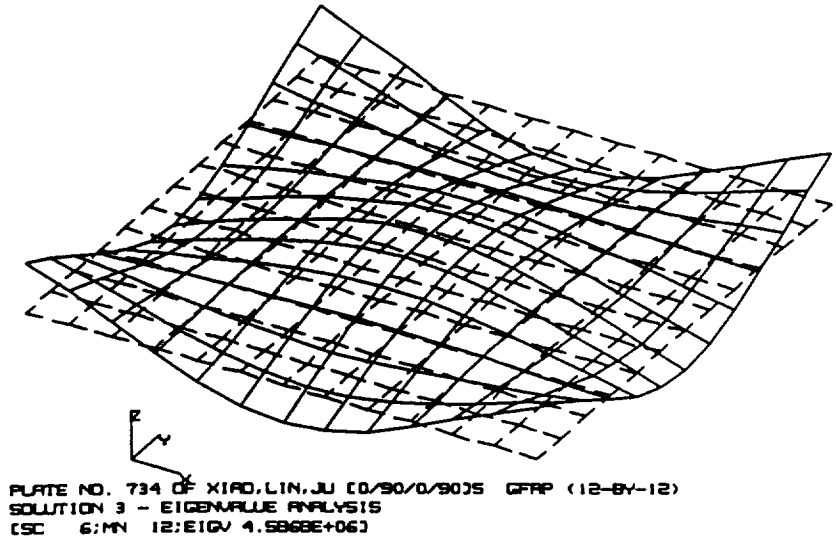

Fig. 3f. Plate 734, Mode 6

Figure 3. (Continued)

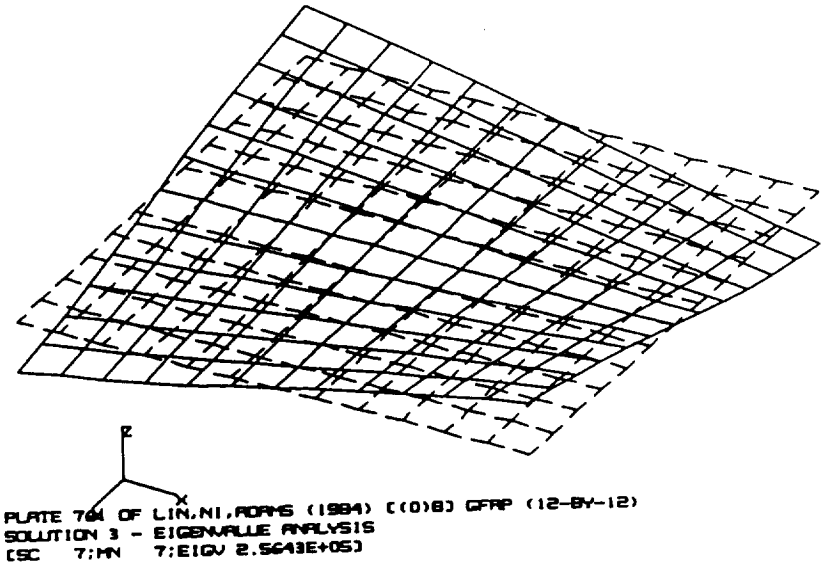

Fig. 4a. Plate 761L, Mode 1

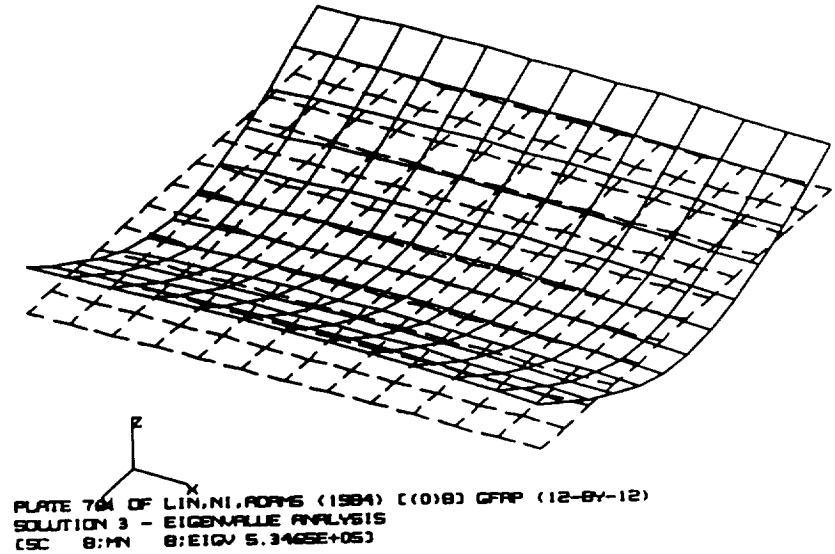

Fig 4b. Plate 761L, Mode 2

Figure 4. NASTRAN-computed eigenmodes for plate 761L

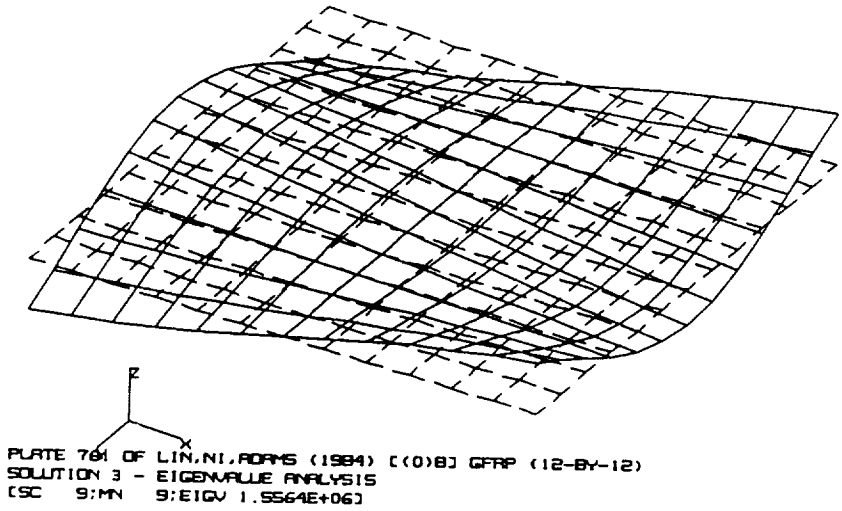

Fig. 4c. Plate 761L, Mode 3

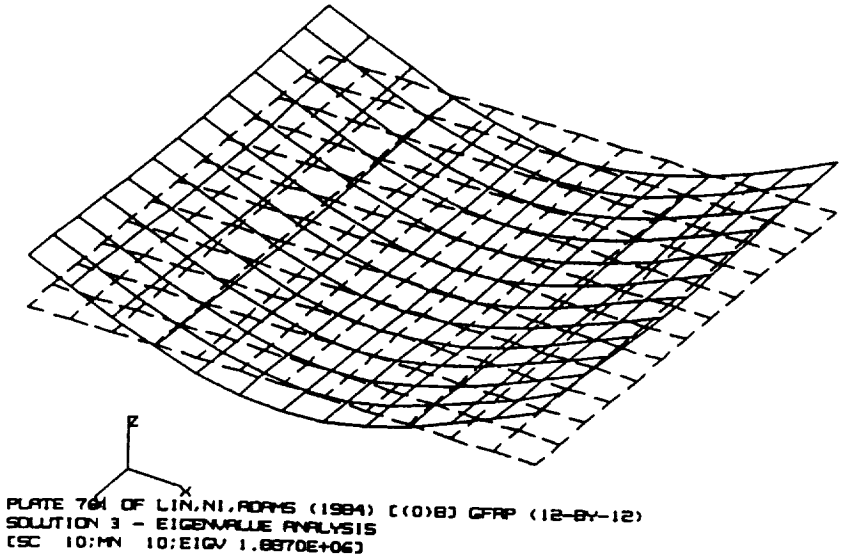

Fig. 4d. Plate 761L, Mode 4

Figure 4. (Continued)

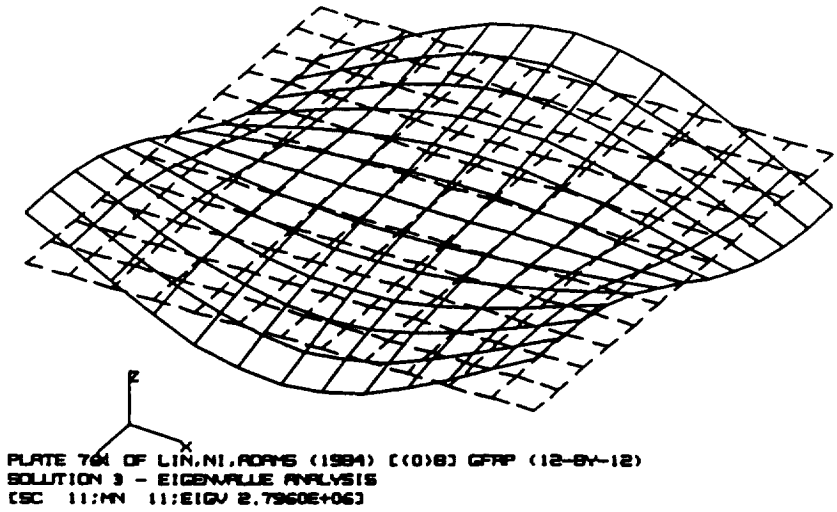

Fig. 4e. Plate 761L, Mode 5

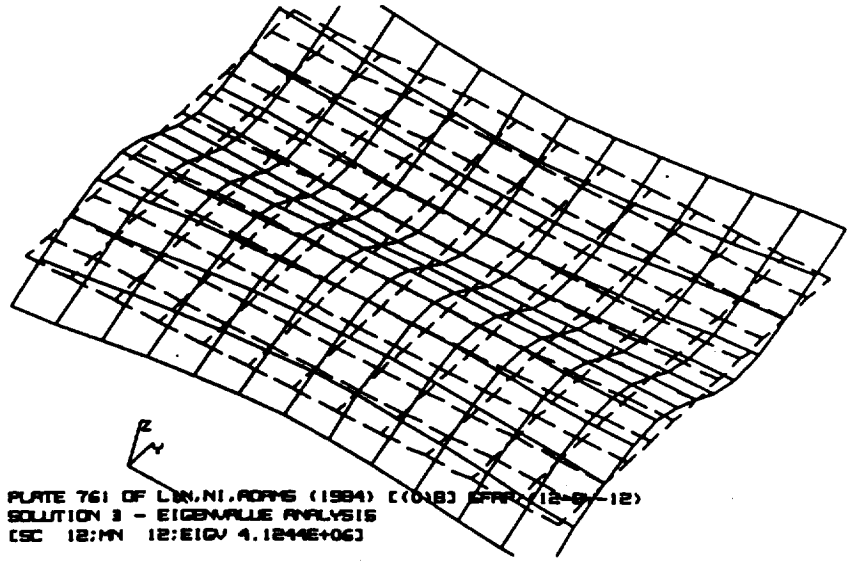

Fig. 4f. Plate 761L, Mode 6

Figure 4. (Continued)

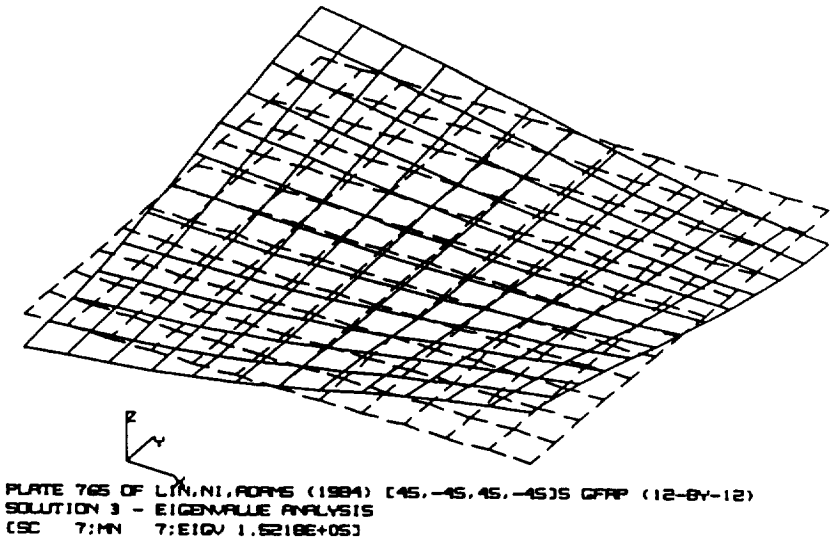

Fig. 5a. Plate 765, Mode 1

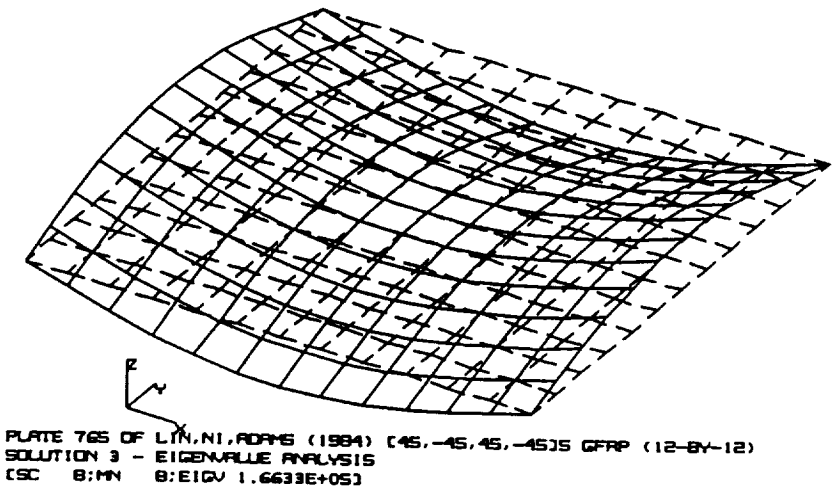

Fig 5b. Plate 765, Mode 2

Figure 5. NASTRAN-computed eigenmodes for plate 765

C2

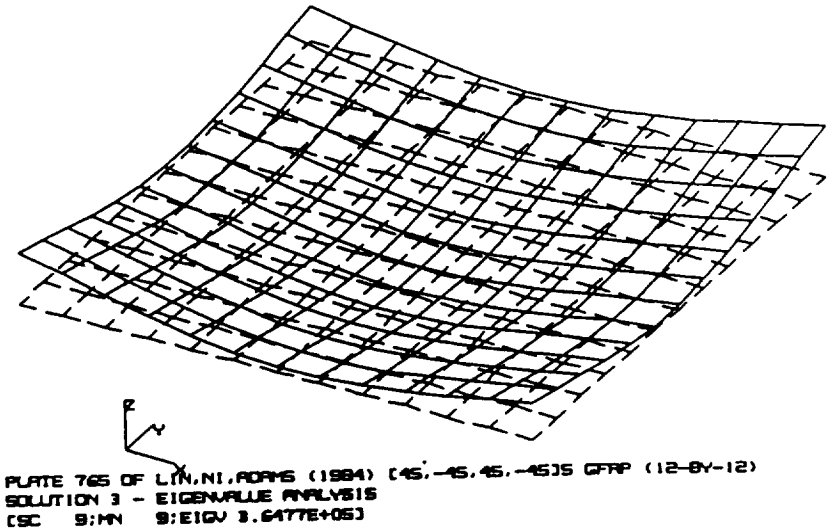

Fig. 5c. Plate 765, Mode 3

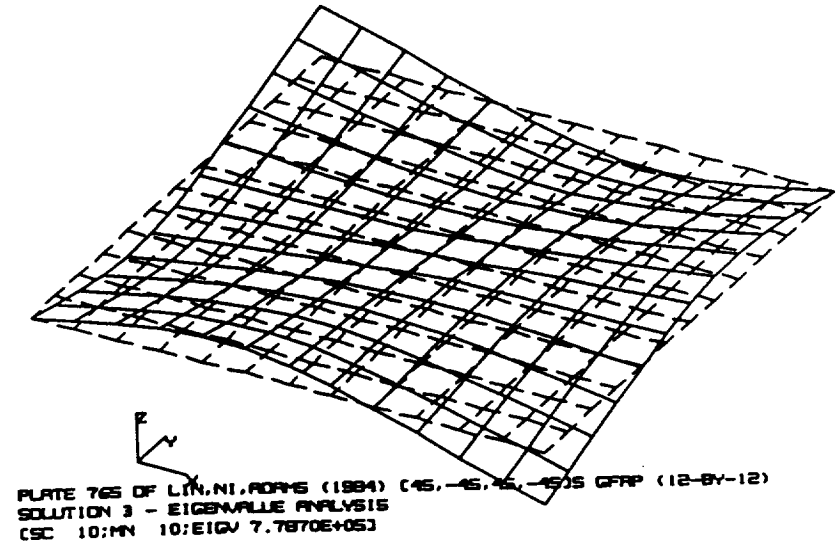

Fig. 5d. Plate 765, Mode 4

Figure 5. (Continued)

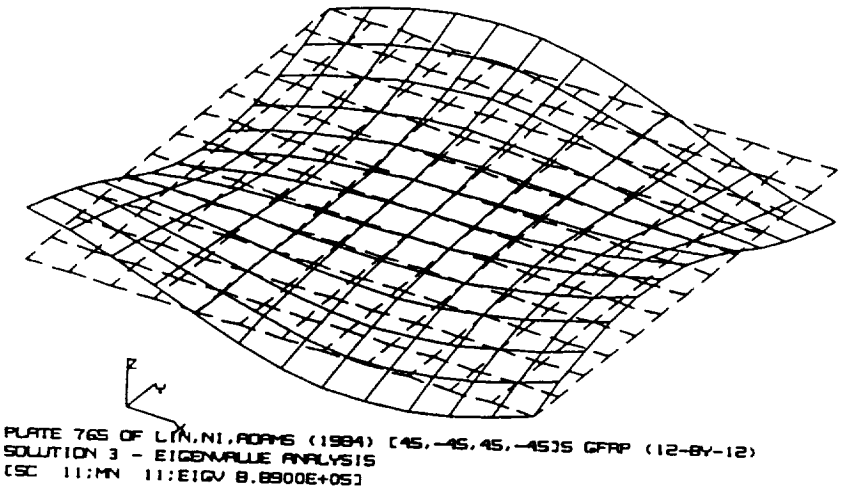

Fig. 5e. Plate 765, Mode 5

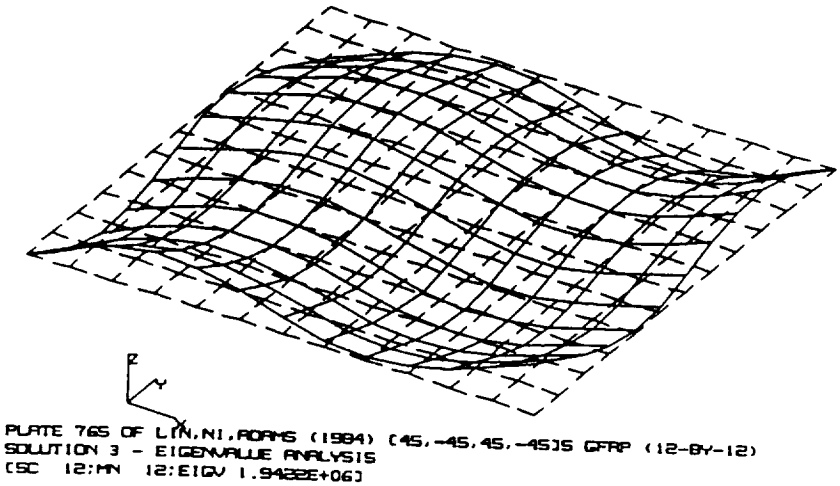

Fig. 5f. Plate 765, Mode 6

Figure 5. (Continued)

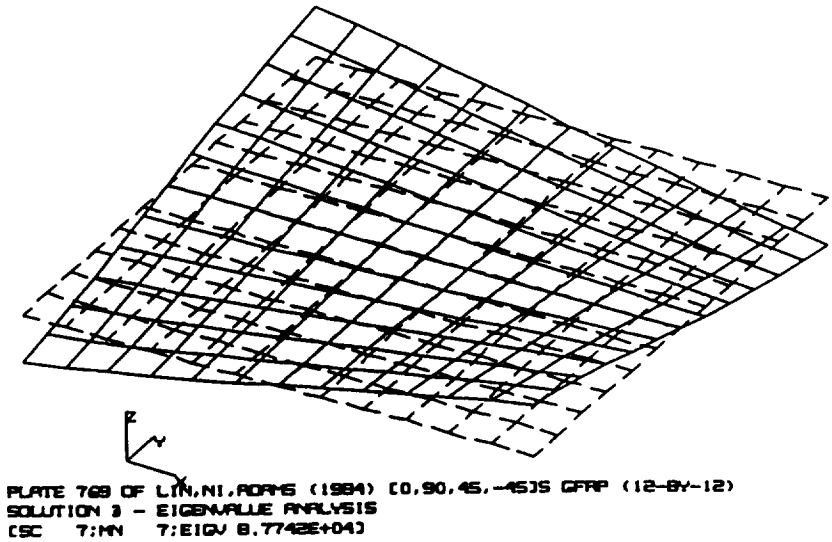

Fig. 6a. Plate 769, Mode 1

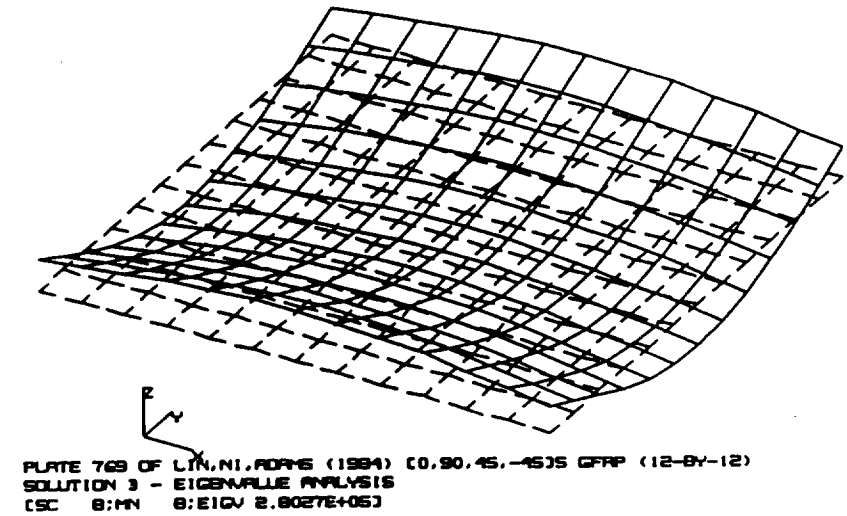

Fig 6b. Plate 769, Mode 2

Figure 6. NASTRAN-computed eigenmodes for plate 769

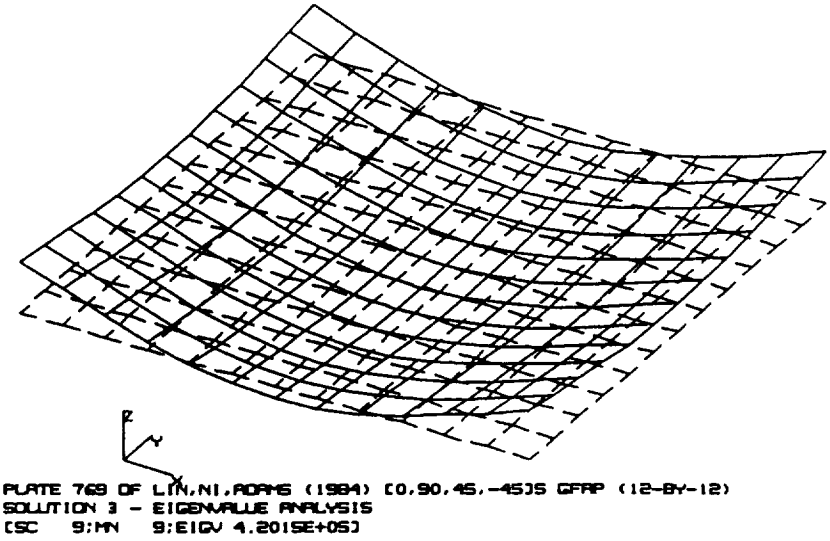

Fig. 6c. Plate 769, Mode 3

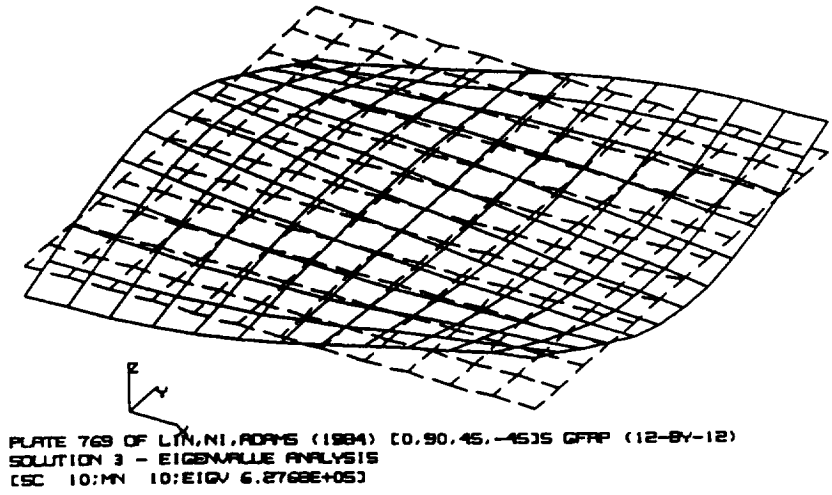

Fig. 6d. Plate 769, Mode 4

Figure 6. (Continued)

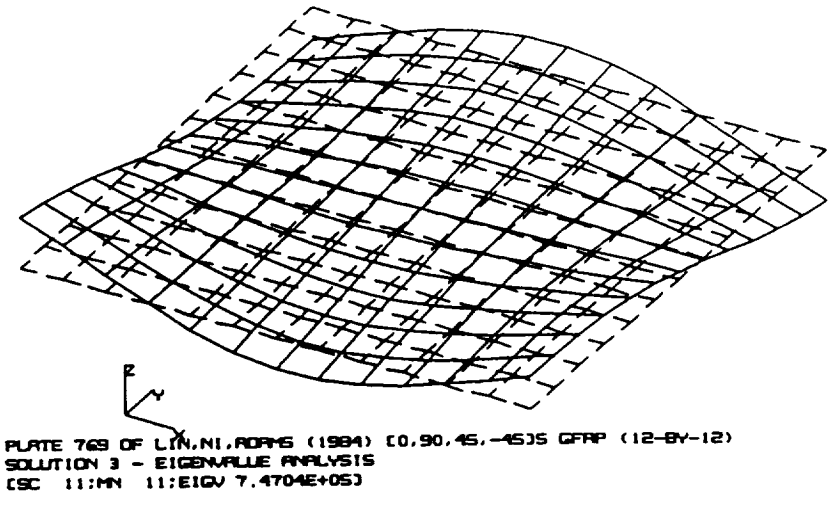

Fig. 6e. Plate 769, Mode 5

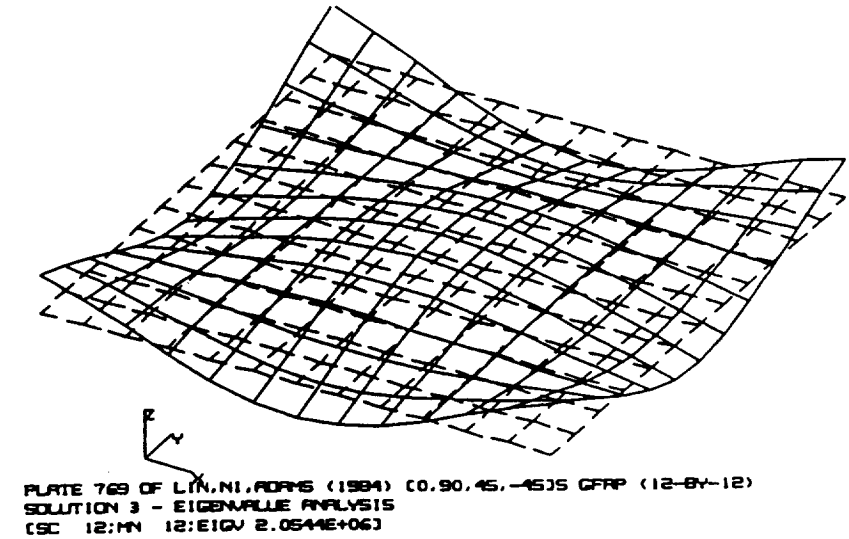

Fig. 6f. Plate 769, Mode 6

Figure 6. (Continued)

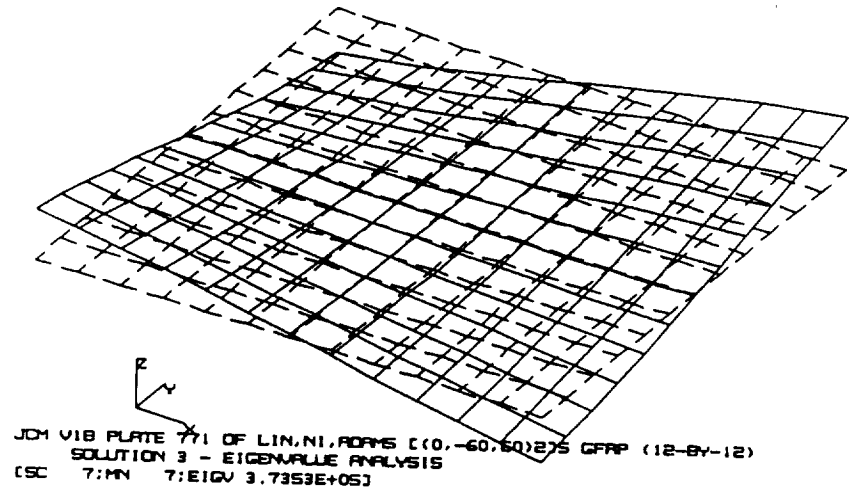

Fig. 7a. Plate 771, Mode 1

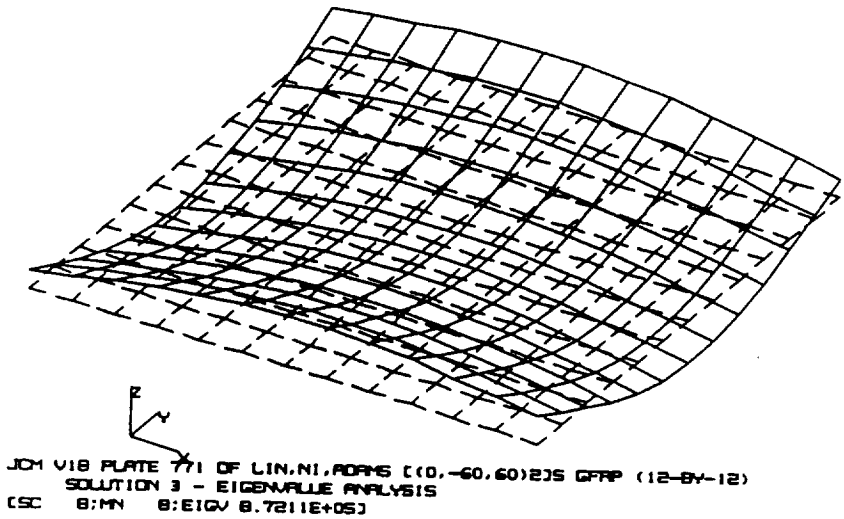

Fig 7b. Plate 771, Mode 2

Figure 7. NASTRAN-computed eigenmodes for plate 771

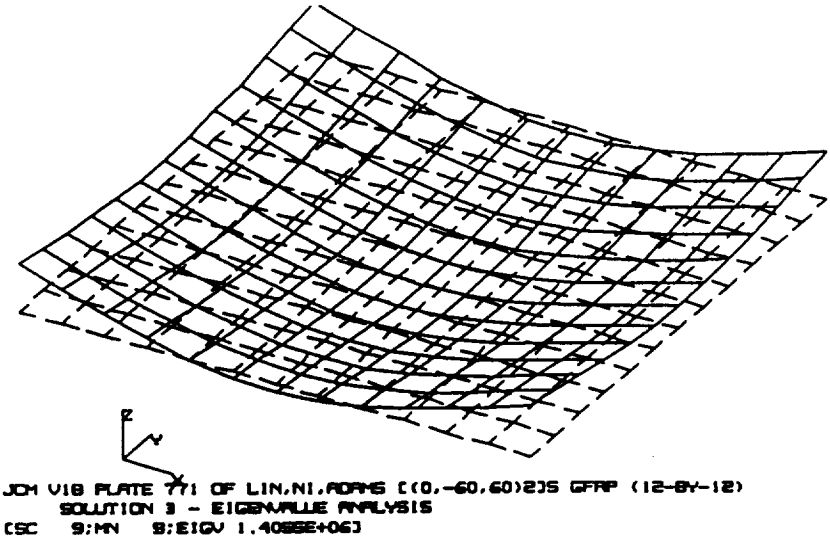

Fig. 7c. Plate 771, Mode 3

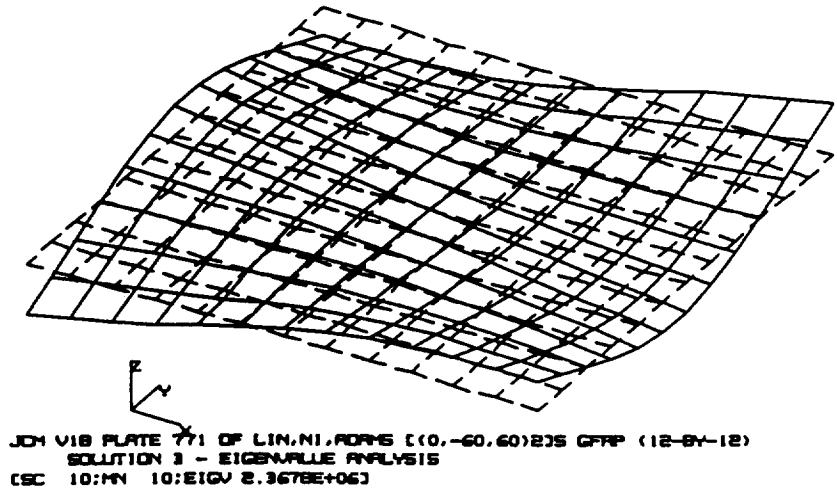

Fig. 7d. Plate 771, Mode 4

Figure 7. (Continued)

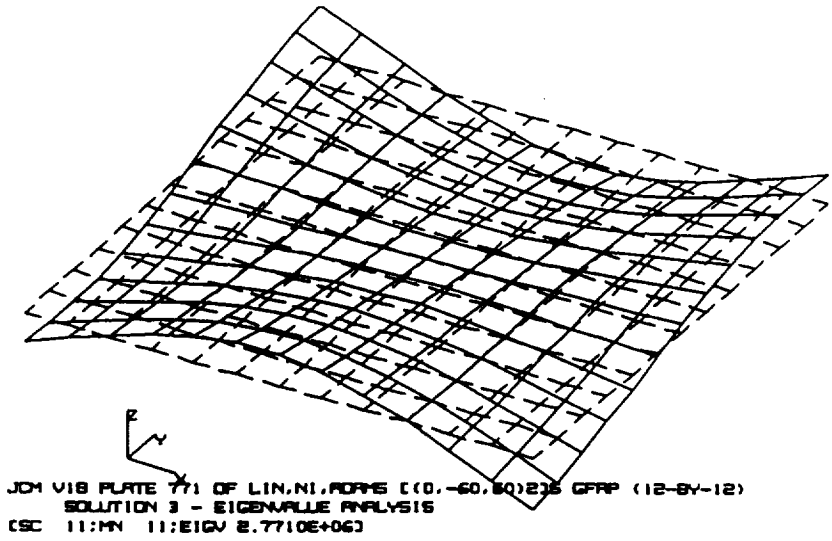

Fig. 7e. Plate 771, Mode 5

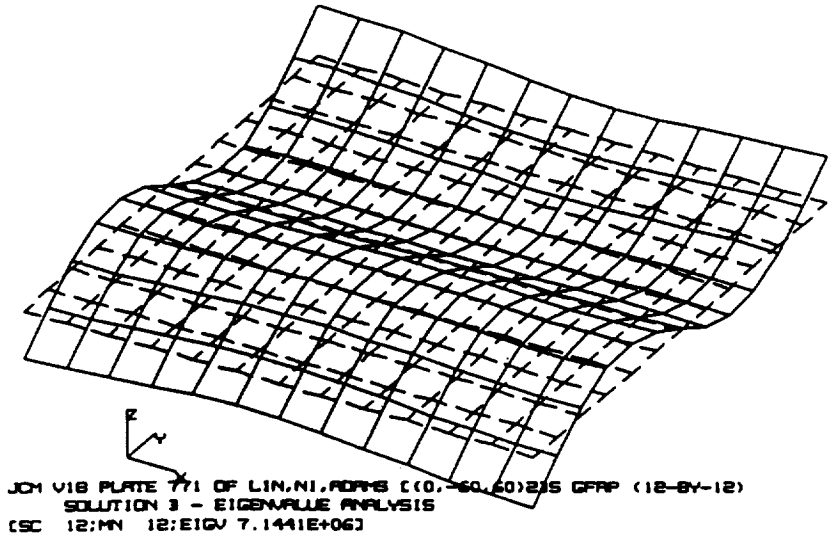

Fig. 7f. Plate 771, Mode 6

Figure 7. (Continued)

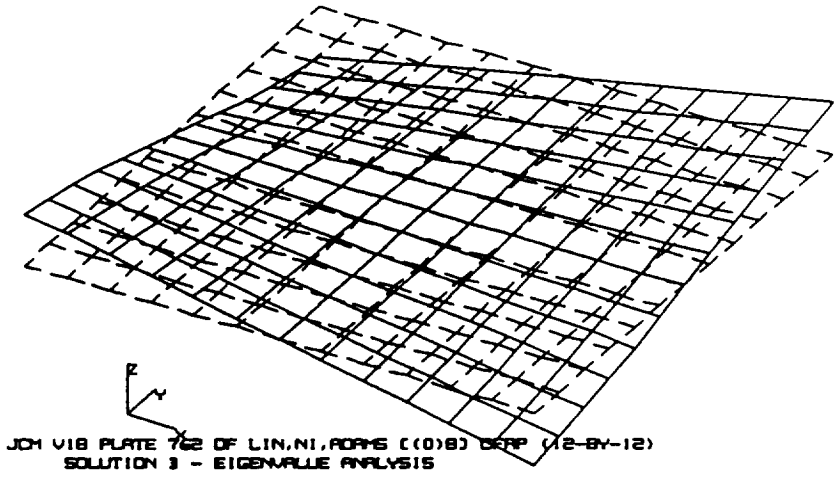

Fig. 8a. Plate 762, Mode 1

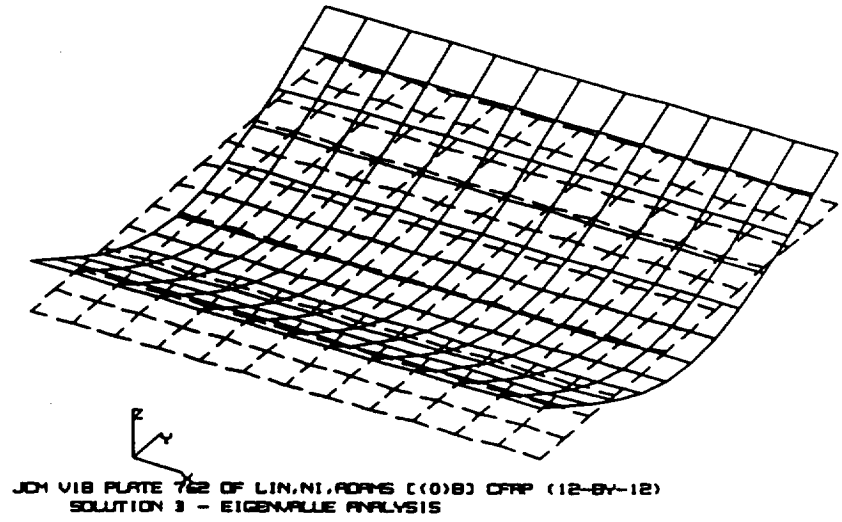

Fig 8b. Plate 762, Mode 2

Figure 8. NASTRAN-computed eigenmodes for plate 762

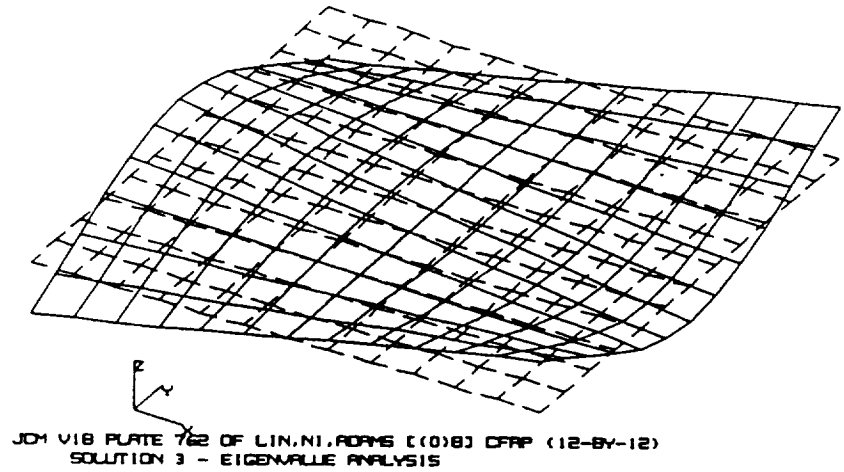

Fig. 8c. Plate 762, Mode 3

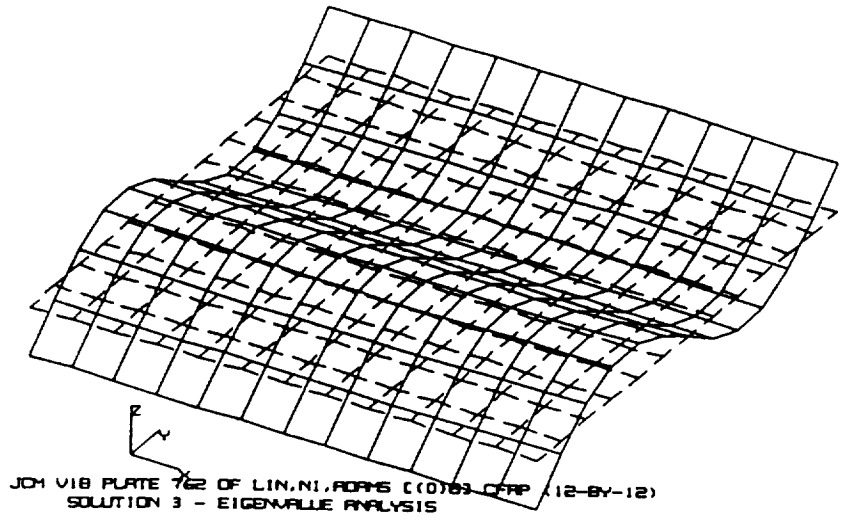

Fig. 8d. Plate 762, Mode 4

Figure 8. (Continued)

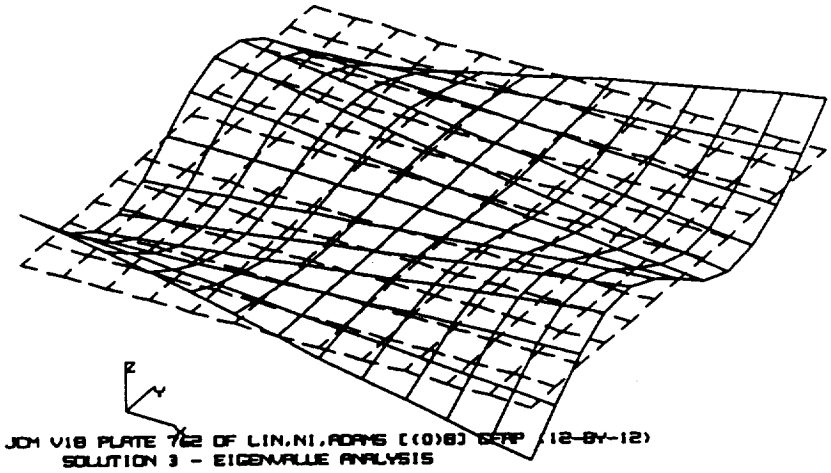

Fig. 8e. Plate 762, Mode 5

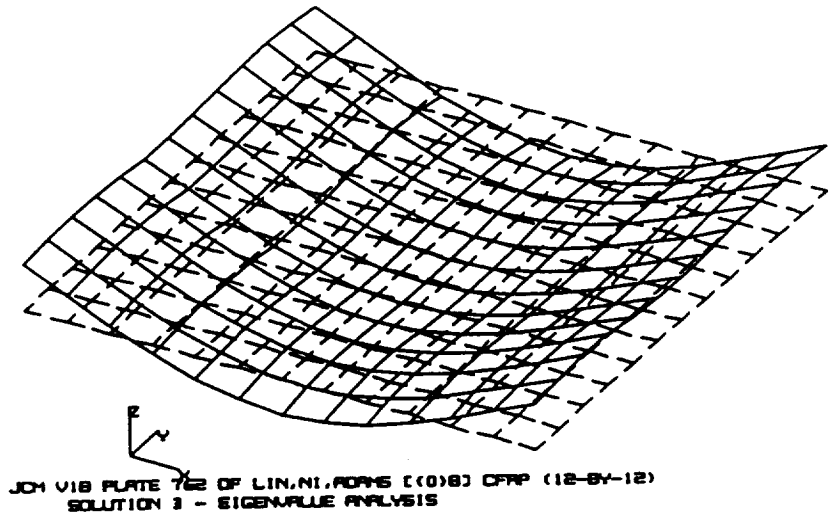

Fig. 8f. Plate 762, Mode 6

Figure 8. (Continued)